CHAPTER IV

RESULTS AND DISCUSSION

1. Isolation and identification of bacteria

Three marine bateria (Sc004, Sc018, and Sc026) were collected around Sichang Island (at 15 m depth). The strain Sc004 was isolated from seawater, while the strains Sc018 and Sc026 were isolated from marine sediments. The characteristics of these strains were determined by the method as described by Barrow and Feltham, 1993. These strains were gram-positive and motiled by peritrichous flagella. The strains Sc018 and Sc026 were subterminal endospore-forming rods, whereas the strain Sc004 was non-spore-forming rod. Colonies on MA plates were opaque, circular, raised with entired edge but showed different colors. The colonies of Sc018, Sc026, and Sc004 showed pale brown, white and yellow colors, repectively. Morphological, cultural, physiological, and biochemical characteristics of three marine bacteria are shown in Table 12. They were deposited at the Department of Microbiology, Faculty of Pharmaceutical Sciences, Chulalongkorn University, Bangkok, Thailand.

สถาบันวิทยบริการ
จุฬาลงกรณ์มหาวิทยาลัย

Table 9. General characteristics of three marine bacteria

Characteristics	Sc018	Sc026	Sc004
gram reaction	+	+	+
cell shape	rod	rod	rod
cell size (μm)	0.4-0.8 x 1.8-4.0	0.5-0.8 x 1.8-3.0	0.4-0.5 x 0.8-2.0
spore position	subterminal	subterminal	-
flagella	peritrichous	peritrichous	peritrichous
motility	+	+	+
catalase	+	+	+
oxidase	+	+	-
urease	-	-	-
MR test	-	-	-
OF test	oxidation	fermentation	oxidation
Voges-Proskauer test	-	+	-
hydrolysis of :			
casein	+++	++	++
hippurate	-	-	-
starch	+++	+++	-
citrate utilization	-	-	-
indole production	-	-	-
nitrate reduction	-	++	+
human blood hemolysis	-	-	-
growth at temperature :			
0.6°C	-	-	-
30°C	+++	+++	+++
37°C	+++	+++	+++
42°C	++	++	++
50°C	-	-	-
growth in NaCl :			
0%	++	++	++
2%	+++	+++	+++
4%	+++	+++	+++
6%	+++	+++	+++
8%	+++	+++	+++
10%	+	-	-
acid produced from :			
L-arabinose	-	-	+++
D-(+)-cellobiose	+++	+++	+++
D-(-)-fructose	+++	+++	+++
D-galactose	-	-	+++
D-glucose	++	+++	+++
inositol	++	++	+++
lactose	+++	-	-
maltose	+++	-	+++
D-mannitol	-	-	+++

Table 9. (continued)

Characteristics	Sc018	Sc026	Sc004
D-(+)-mannose	-	-	+++
melibiose	-	-	+++
melizitose	-	-	+++
L-rhamnose	-	-	+++
raffinose	++	++	+++
D-(-)-ribose	-	-	-
salicin	+++	+++	+++
sorbitol	+++	+++	+++
sorbose	+	-	+++
sucrose	-	+++	+++
D-(+)-trehalose	++	++	+++
D-(+)-xylose	-	-	+++
G+C content (mol%)	37.4	ND	ND

+, Positive reaction; -, Negative reaction; ND, Not determined.

Figure 6. Scanning electron micrograph of Sc018

Figure 7. Scanning electron micrograph of Sc026

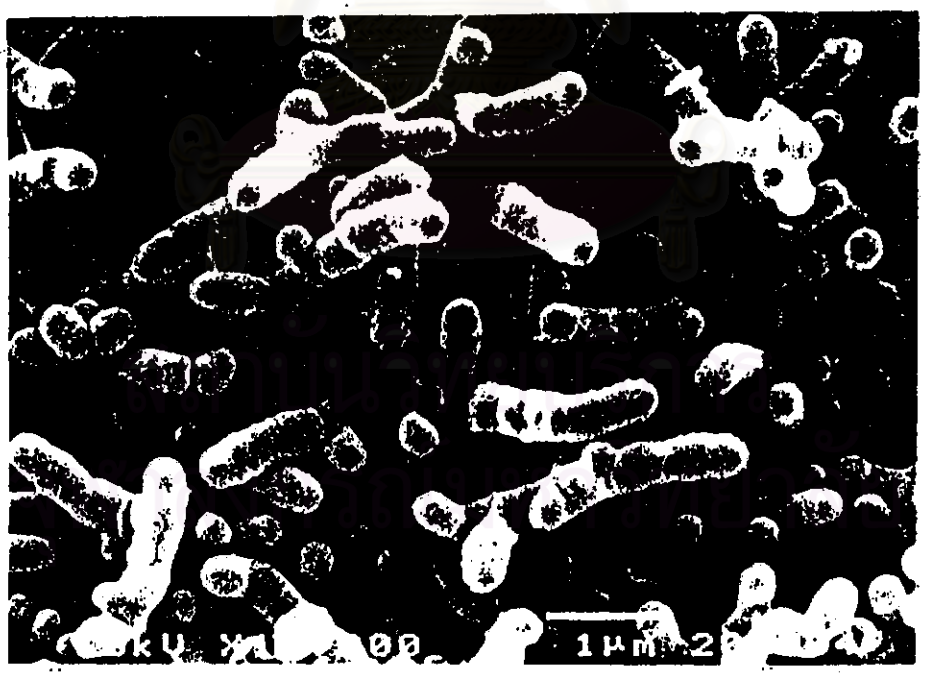

Figure 8. Scanning electron micrograph of Sc004

On the basis of these available characteristics (Table 9), the strains Sc018 and Sc026 were identified as *Bacillus* (Berkeley, and Claus, 1989, and Shida *et al.*, 1997), whereas the strain Sc004 was left unidentified. The species of *Bacillus* strains Sc018 and Sc026 could not be identified by comparison of the morphological and biochemical characteristics of these strains with those of many known species of *Bacillus* (Tables 2 and 9).

2. Structure elucidation of isolated compounds

Thirteen compounds were isolated from three marine bacteria are described in Table 10. Most of them were isolated from a marine *Bacillus* sp. Sc026.

Table 10. Chemical compounds elaborated by marine bacteria Sc004, Sc018, and Sc026

Number	Compounds	Weight (mg)	Codes	Sources
1	*cyclo*-(L-prolyl-glycyl)	4	P056WC	Sc026
		110	P056YEL	
		353	S142	Sc004
		67	S151	
2	*cyclo*-(D-prolyl-leucyl)	5	F019	Sc018
3	*cyclo*-(L-prolyl-D-leucyl)	12	P049	Sc026
		6	P193WC	
4	*cyclo*-(D-prolyl-isoleucyl)	3	F017	Sc018
5	*cyclo*-(D-prolyl-L-phenylalanyl)	13	P348	Sc026
6	*cyclo*-(*trans*-4-hydroxy-L-prolyl-L-phenylalanyl)	31	F018	Sc018

Table 10. (continued)

Number	Compounds	Weight (mg)	Codes	Sources
7	*cyclo*-(L-prolyl-L-tryptophanyl)	4	P350	Sc026
8	*cyclo*-(D-prolyl-L-tryptophanyl)	5	P352	
9	2'-deoxyadenosine	20	S147	Sc004
10	macrolactin F	65	P035	Sc026
11	7-*O*-succinyl macrolactin F	7	P129	
12	7-*O*-succinyl macrolactin A	28	P103	
13	*cyclo*-(4-hydroxy-prolyl-4-hydroxy-prolyl-leucyl-phenylalanyl)	13	P132	Sc026

2.1 *Cyclo*-(L-prolyl-glycyl) (P056WC, P056YEL, S142, and S151)

The ESITOF mass spectrum of compound S151 (Figure 30) showed the pseudo molecular ion peak at *m/z* 155 $(M+H)^+$ implying a molecular formula of $C_7H_{10}N_2O_2$. The UV spectrum (Figure 31) exhibited λ_{max} (log ϵ) at 205 (3.81) and 271 (0.18) nm, and the IR spectrum (Figure 32) suggested the presence of amide NH (ν_{max} 3207 cm^{-1}), cycloalkane (ν_{max} 2922 cm^{-1}), and amide carbonyl (ν_{max} 1651 cm^{-1}) groups.

As seen on the 300 MHz ^1H NMR (in DMSO-d_6) of compound S151 (Figure 33), there were five methylene proton signals at δ 1.75-1.85 (3H), 2.21 (1H), 3.33 (1H), 3.49 (1H), 3.98 (1H) ppm, one methine proton signal (δ 4.11 ppm), and one amide proton signal (δ 8.06 ppm). The 75 MHz ^{13}C NMR spectrum (in DMSO-d_6) of compound S151 (Figure 34) showed seven carbon signals attributable to two quaternary carbons (δ 163.7, 169.1

ppm), one methine carbon (δ 58.1 ppm), and four methylene carbons (δ 22.3, 28.1, 44.8, 46.1 ppm) as determined by the DEPT 135 spectrum (Figure 35).

According to the HMQC spectrum of compound S151 (Figure 36), the protonated carbons could be assigned as follows: 2H-3 (δ 3.49, 3.98 ppm)-C-3 (δ 46.1 ppm), H-6 (δ 4.11 ppm)-C-6 (δ 58.1 ppm), 2H-7 (δ 1.75-1.85, 2.21 ppm)-C-7 (δ 28.1 ppm), 2H-8 (δ 1.75-1.85 ppm)-C-8 (δ 22.3 ppm), and 2H-9 (δ 3.33 ppm)-C-9 (δ 44.8 ppm).

The ^{1}H-^{1}H COSY spectrum (Figure 37) of compound S151 exhibited the correlations as follows: 2H-3 (δ 3.49 ppm) to 4-NH (δ 8.06 ppm), H-6 (δ 4.11 ppm) to 2H-7 (δ 1.75-1.85, 2.21 ppm), and H_b-7 (δ 2.21 ppm) to 2H-8 (δ 1.75-1.85 ppm), 2H-8 to 2H-9 (δ 3.33 ppm).

The complete carbon assignment of compound S151 was achieved by the analysis of the HMBC ($^{n}J_{HC}$ = 8 Hz) spectrum (Figure 38). The amide carbonyl carbon signal (δ 163.7 ppm) was assigned as C-2 by the long-range correlation with 2H-3 (δ 3.49, 3.98 ppm). The HMBC spectra also showed the correlations of 2H-7 (δ 1.82, 2.21 ppm) to C-8 (δ 22.3 ppm) and 2H-8 (δ 1.75-1.85 ppm) to C-9 (δ 44.8 ppm). The correlations from the HMBC spectral data were shown in Figure 9.

The ^{1}H and ^{13}C NMR spectral data of compounds P056WC, P056YEL, and S142 were identical to those of compound S151, it is therefore concluded that they are the same substance. In addition, all compounds showed similar optical rotations ($[\alpha]^{25}_{D}$ −68.8°,

-41.0°, -13.2°, and -78.5°, c = 0.14, (MeOH) for compounds P056WC, P056YEL, S142, and S151, respectively).

The ^{1}H and ^{13}C NMR spectral data of compound S151 (Table 11) were similar to a diketopiperazine compound, *cyclo*-(L-prolyl-glycyl) previously isolated from the starfish, *Luidia clathrata* (Pettit *et al.*, 1973), the sponge, *Geodia baretti* (Lidren, and Behlin, 1986), and the marine bacterium, *Alteromonas* sp. S9730 (Thongton, 1998). Therefore, compound S151 was identified as *cyclo*-(L-prolyl-glycyl).

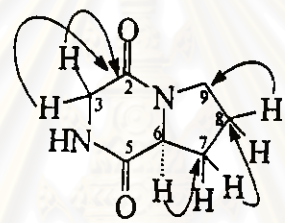

Figure 9. The long-range correlations in the HMBC spectrum of *cyclo*-(L-prolyl-glycyl) (S151)

Table 11. ^{1}H and ^{13}C NMR spectral data of compound S151 (in DMSO-d_6) and *cyclo*-(L-prolyl-glycyl) (in $CDCl_3$)

Position	*Cyclo*-(L-prolyl-glycyl) (S151)[a]		*Cyclo*-(L-prolyl-glycyl)[b]	
	δ_C(ppm)	δ_H(ppm), mult. (*J* in Hz)	δ_C(ppm)	δ_H(ppm), mult. (*J* in Hz)
2	163.7	-	169.7	-
3a	46.1	3.49, dd (3.8, 16.6)	46.6	3.89, dd (4.4, 16.4)
3b		3.98, d (16.6)		4.08, d (16.1)
4	-	8.06, NH, br s	-	6.34, NH, br

Table 11. (continued)

Position	*Cyclo*-(L-prolyl-glycyl) (S151)[a]		*Cyclo*-(L-prolyl-glycyl)[b]	
	δ_C(ppm)	δ_H(ppm), mult. (*J* in Hz)	δ_C(ppm)	δ_H(ppm), mult. (*J* in Hz)
5	169.1	-	163.4	-
6	58.1	4.11, dd (3, 8)	58.5	4.11, br t
7a	28.1	1.75-1.85, m[c]	28.5	1.97-2.07, m[c]
7b		2.21. m		2.19, m
8a	22.3	1.75-1.85, 2H, m[c]	22.4	1.97-2.07, m[c]
8b				1.91, m
9	44.8	3.33, 2H, m	45.3	3.52-3.64, 2H, m

[a]Data were recorded at 300 MHz (^{1}H) and 75 MHz (^{13}C).
[b] *Cyclo*-(L-prolyl-glycyl) from Thongton, 1998.
[c]Overlapping signal.

2.2 *Cyclo*-(L-prolyl-D-leucyl) (P049 and P193WC) and *cyclo*-(D-prolyl-leucyl) (F019)

The chemical ionization mass spectra of compounds P049 and F019 (Figures 39 and 51) showed the pseudomolecular ion peak at *m/z* 211 $(M+H)^+$ implying the molecular formula of $C_{11}H_{18}N_2O_2$. The UV spectra exhibited λ_{max} (log ϵ) at 205 (3.58) and 272 (0.33) nm for compound P049 (Figure 40) and at 205 (3.85) and 272 (0.31) nm for compound F019 (Figure 52). The IR spectra of compounds P049 and F019 (Figures 41 and 53) confirmed the presence of amide NH (ν_{max} 3257 cm^{-1} for compound P049 and 3298 cm^{-1} for compound F019), cycloalkane (ν_{max} 2950 cm^{-1} for compound P049 and 2959 cm^{-1} for compound F019),

and amide carbonyl (ν_{max} 1664, 1633 cm^{-1} for compound P049 and 1667 cm^{-1} for compound F019) groups.

The 300 MHz ^1H NMR spectra (in $CDCl_3$) of compounds P049 and F019 (Figures 42 and 54 and Table 12) were almost identical. The proton resonances slightly differed at 2H-9 (δ 3.52 ppm of compound P049 and δ 3.46, 3.58 ppm of compound F019), and 2H-10 (δ 1.50, 1.99 ppm of compound P049 and δ 1.58 ppm of compound F019). The 75 MHz ^{13}C NMR spectra (in $CDCl_3$) of compounds P049 and F019 (Figures 43 and 55 and Table 12) were also almost identical except that C-3 and C-10 (δ 53.4 and 38.6 ppm) of compound P049 were more upfield than C-3 and C-10 (δ 56.5 and 42.8 ppm) of compound F019. The DEPT 135 spectra in $CDCl_3$ of compounds P049 and F019 (Figures 44 and 56) exhibited two methyl carbon signals, four methylene carbon signals, and three methine carbon signals.

The HMQC spectra of compounds P049 and F019 (Figures 45-48 and 57-58) allowed the assignment of protons and their respective carbons, as shown in Table 12. Similar ^1H-^1H correlations in the ^1H-^1H COSY spectra of compounds P049 and F019 (Figures 46-47 and 57) established the proton connectivities as follows: H-3, 2H-10, H-11, 3H-12, and 11-Me; H-6, 2H-7, 2H-8 and 2H-9.

The complete carbon assignment of compound P049 was achieved by the analysis of the HMBC ($^nJ_{HC}$ = 8 Hz) spectrum (Figures 49 and 50). The HMBC spectral data demonstrated correlations of 2H-10 (δ 1.50, 1.99 ppm) to C-2 (δ 170.0 ppm), C-3 (δ 53.4

ppm) and C-12 (δ 23.4 ppm); H-11 (δ 1.79 ppm) to C-11-Me (δ 21.3 ppm) and C-12 (δ 23.4 ppm); and 2H-7 (δ 2.10, 2.32 ppm) to C-8 (δ 22.8 ppm).

Compounds P049 and F019 were then proposed as the diketopiperazine, *cyclo*-(prolyl-leucyl). A series of *cyclo*-(prolyl-leucyl) diketopiperazines were previously reported as follows: *cyclo*-(prolyl-leucyl) from a marine *Micrococcus* sp. associated with a marine sponge, *Tedania ignis* (Stierle, Cardellina, and Singleton, 1988); *cyclo*-(L-prolyl-D-leucyl) and *cyclo*-(D-prolyl-D-leucyl) from a Carribbean sponge, *Calyx* cf. *podatypa* (Adamczeski, Reed, and Crews, 1995); and *cyclo*-(L-prolyl-L-leucyl) from a terrestrial *Streptomyces* sp. (Johnson, Jackson, and Eble, 1951), an algae *Scenedesmus* sp. (Luedemann *et al.*, 1961), and an Antartic sponge-associated bacterium, *Pseudomonas aeruginosa* (Jayatilake *et al.*, 1996).

The difference of some proton and carbon chemical shifts and of their optical rotations ($[\alpha]^{25}_{D}$ –91.3° and +13.6°, c = 0.14, (MeOH) for compounds P049 and F019, respectively) indicated their stereochemistry difference. The absolute stereochemistry of *cyclo*-(L-prolyl-D-leucyl) and *cyclo*-(D-prolyl-D-leucyl) were previously identified by comparing optical rotations with known proline-containing diketopiperazines (Adamczeski, Reed, and Crews, 1995), while the absolute stereochemistry of *cyclo*-(L-prolyl-L-leucyl) was identified by acid hydrolysis and R_f values of amino acids on chiral TLC plates (Jayatilake *et al.*, 1996). Generally, it is well known that optical rotations for proline-containing diketopiperazines are positive if proline of diketopiperazines is D-proline, while showing negative if the proline is L-proline (Adamczeski, Reed, and Crews, 1995). Optical rotations

($[\alpha]^{25}_{D}$) of compounds P049 and F019 were –91.3 and +13.6°, respectively; it is therefore concluded that compounds P049 and F019 contained L-prolyl and D-prolyl subunits in the structures, respectively. Compound P049 was then identified as *cyclo*-(L-prolyl-D-leucyl) which was confirmed by comparison its ^{1}H, ^{13}C NMR spectral data and optical rotation with the previously reported *cyclo*-(L-prolyl-D-leucyl) (Adamczeski, Reed, and Crews, 1995) as shown in Tables 12, 13 and 14. The ^{1}H, ^{13}C NMR spectral data, and optical rotation of compound P193WC were identical to those of compound P049, *cyclo*-(L-prolyl-D-leucyl) as shown in Tables 12, 13 and 14. The ^{1}H and ^{13}C NMR spectral data of compound F019 were similar to those of *cyclo*-(D-prolyl-D-leucyl) as shown in Tables 12 and 13, so it might be *cyclo*-(D-prolyl-D-leucyl).

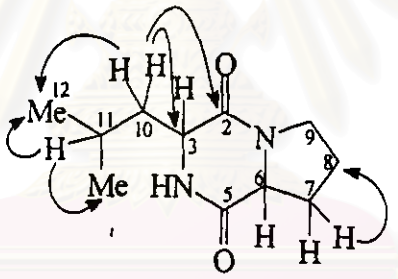

Figure 10. The long-range correlations in the HMBC spectra of *cyclo*-(L-prolyl-D-leucyl) (P049 and P193WC) and *cyclo*-(D-prolyl-leucyl) (F019)

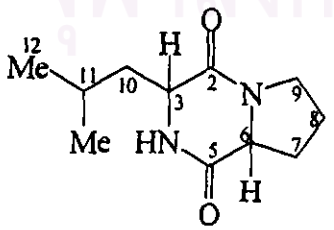

Figure 11. *Cyclo*-(prolyl-leucyl)

Compounds	H-3	H-6
cyclo-(D-prolyl-L-leucyl)	β	α
cyclo-(L-prolyl-D-leucyl)	β	β
cyclo-(D-prolyl-D-leucyl)	α	β
cyclo-(L-prolyl-L-leucyl)	β	α

Table 12. ^{1}H and ^{13}C NMR spectral data of *cyclo*-(L-prolyl-D-leucyl) (P049) and *cyclo*-(D-prolyl-leucyl) (F019) (in $CDCl_3$)

Position	*Cyclo*-(L-prolyl-D-leucyl) (P049)[a]		*Cyclo*-(D-prolyl-leucyl) (F019)[a]	
	δ_C (ppm)	δ_H (ppm), mult. (*J* in Hz)	δ_C (ppm)	δ_H (ppm), mult. (*J* in Hz)
2	166.0	-	166.8	-
3	53.4	3.95, dd (3.3, 9.3)	56.5	3.87, m
4	-	6.18, br s	-	6.22, br s
5	170.0	-	169.3	-
6	59.0	4.11, t (8.1)	58.0	4.02, t (7.0)
7a	28.2	2.10, m	29.0	1.94, m
7b		2.32, m		2.33, m
8a	22.8	1.89, 2H, m	22.3	1.89, m
8b				1.98, m
9a	45.5	3.52, 2H, m	45.5	3.46, m
9b				3.58, m
10a	38.6	1.50, m	42.8	1.58, 2H, m
10b		1.99, m		
11	24.7	1.79, m	24.2	1.75, m
11-Me[b]	21.3	0.90, 3H, d (6.3)	21.1	0.88, 3H, d (6.3)
12[b]	23.4	0.95, 3H, d (6.3)	23.0	0.92, 3H, d (6.3)

[a]Data were acquired at 300 MHz (^{1}H) and 75 MHz (^{13}C).
[b]Assignments may be interchangeable.

Table 13. ^{1}H and ^{13}C NMR spectral data of *cyclo*-(L-prolyl-D-leucyl), *cyclo*-(L-prolyl-L-leucyl), and *cyclo*-(D-prolyl-D-leucyl) (in $CDCl_3$)

Position	*Cyclo*-(L-prolyl-D-leucyl)[a]		*Cyclo*-(L-prolyl-L-leucyl)[b]	*Cyclo*-(D-prolyl-D-leucyl)[a]	
	δ_C (ppm)	δ_H (ppm), mult. (*J* in Hz)	δ_C (ppm)	δ_C (ppm)	δ_H (ppm), mult. (*J* in Hz)
2	171.4	-	ND	169.6	-
3	53.4	4.01, dd (3.4, 9.4)	53.6	56.4	3.92, ddd (4.5, 5.4, 9.9)
4	-	5.91, br s	-	-	6.68, br s
5	167.1	-	ND	166.4	-
6	59.1	4.12, t (8.1)	59.2	58.1	4.07, dd (1.5, 6.9)
7a 7b	28.2	2.13, m 2.33, m	28.3	29.1	2.02, m 2.37, ddd (2.4, 6.4, 8.7)
8a 8b	22.8	1.86-1.94, m 1.99-2.02, m	23.5	23.1	1.96, m 1.88, m
9a 9b	45.6	3.5-3.6, 2H, m	45.7	45.7	3.52, dt (2.7, 9.8) 3.62, dt (4.5, 9.0)
10a 10b	38.7	1.52, ddd (4.9, 9.6, 14.5) 2.01, m	38.9	42.6	1.63, ddd (1.8, 6.5, 11.1) 1.75, q (6.3)
11	24.8	1.69-1.76, m	25.0	24.5	1.60-1.66, m (under H-10)
11-Me[c]	21.2	1.00, 3H, d (6.3)	21.4	21.4	0.97, d (6.3)
12[c]	22.8	0.94, 3H, d (6.3)	23.0	22.3	0.94, d (6.3)

[a]*Cyclo*-(L-prolyl-D-leucyl) from Adamczeski, Reed, and Crews, 1995.
[b]*Cyclo*-(L-prolyl-L-leucyl) from Jayatilake *et al.*, 1996.
[c]Assignments may be interchangeable.
ND = No data.

Table 14. Optical rotations of *cyclo*-(L-prolyl-D-leucyl) (P049), *cyclo*-(D-prolyl-leucyl) (F019), *cyclo*-(L-prolyl-D-leucyl), *cyclo*-(D-prolyl-D-leucyl), and *cyclo*-(L-prolyl-L-leucyl)

Compounds	$[\alpha]_D$ (°)	Concentration (g/100 ml)
cyclo-(L-prolyl-D-leucyl) (P049)	-91.3	0.14[c]
cyclo-(D-prolyl-leucyl) (F019)	+13.6	0.14[c]
cyclo-(L-prolyl-D-leucyl)[a]	-90.6	0.14[d]
cyclo-(D-prolyl-D-leucyl)[a]	+142.1	0.28[d]
cyclo-(L-prolyl-L-leucyl)[b]	-136.0	0.12[d]

[a]*Cyclo*-(L-prolyl-D-leucyl) from Adamczeski, Reed, and Crews, 1995.
[b]*Cyclo*-(L-prolyl-L-leucyl) from Jayatilake *et al.*, 1996.
[c]Data were recorded in MeOH.
[d]Data were recorded in EtOH.

สถาบันวิทยบริการ
จุฬาลงกรณ์มหาวิทยาลัย

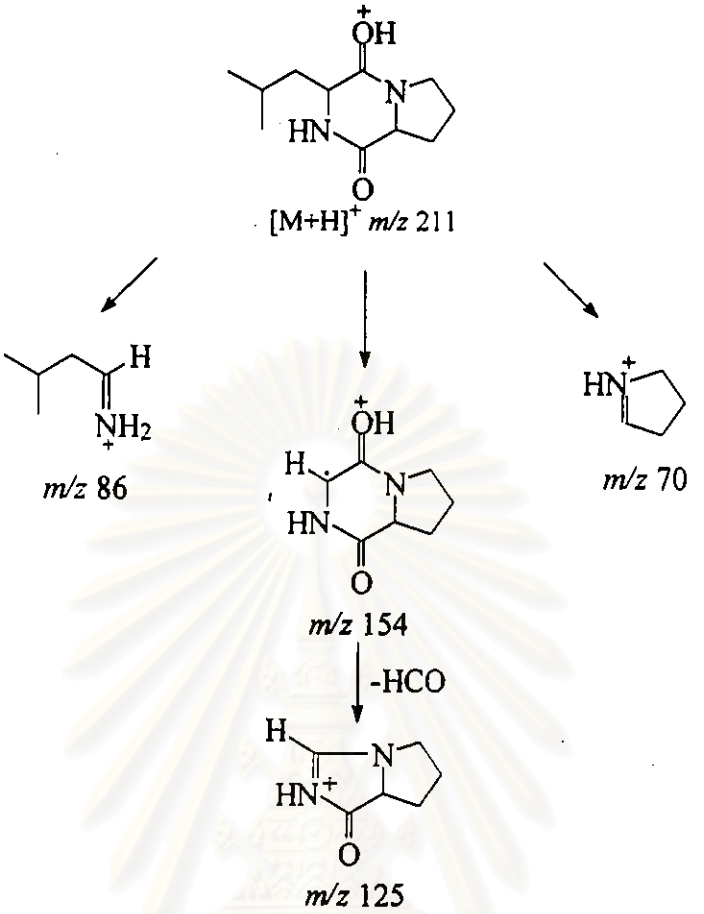

Scheme 6. Proposed mass fragmentation of *cyclo*-(L-prolyl-D-leucyl) (P049) and *cyclo*-(D-prolyl-leucyl) (F019)

สถาบันวิทยบริการ
จุฬาลงกรณ์มหาวิทยาลัย

2.3 *Cyclo*-(D-prolyl-isoleucyl) (F017)

The chemical ionization, mass spectrum of F017 (Figure 59) showed the protonated molecular ion peak at *m/z* 211 $(M+H)^+$ suggesting a molecular formula of $C_{11}H_{18}N_2O_2$. The UV spectrum (Figure 60) exhibited λ_{max} (log ϵ) at 210 (4.36) nm, and the IR spectrum (Figure 61) showed the maximum absorption bands at 3252 cm^{-1} (amide NH streching), 2964 cm^{-1} (cycloalkane streching), and 1673 cm^{-1} (carbonyl streching).

The ^1H NMR (Figure 62), ^{13}C NMR (Figure 63), DEPT 135 (Figure 64), HETCOR (Figure 65) and ^1H-^1H COSY (Figure 66) spectral data of compound F017 assisted in the assignment of both protons and carbons of F017 (Table 15). The spectral data clearly showed the prolyl subunit in compound F017. The absence of two methyl protons as two doublets and the presence of two methyl protons as a doublet and a triplet at δ 0.95 and 0.88 ppm suggested the isoleucyl subunit in compound F017. Therefore compound F017 was proposed as *cyclo*-(prolyl-isoleucyl). The ^1H (Figure 62) and ^{13}C (Figure 63) NMR spectral data (in $CDCl_3$) of compound F017 (Table 15) were found to be similar to the known compound, *cyclo*-(L-prolyl-L-isoleucyl), previously isolated from a Caribbean sponge, *Calyx* cf. *podatypa* (Adamczeski, Reed, and Crews, 1995) and from the Antartic sponge-associated bacterium, *Pseudomonas aeruginosa* (Jayatilake *et al.*, 1996). However the optical rotation of compound F017 ($[\alpha]^{25}_D$ +25.8°, c = 0.14 (MeOH)) was different from that of known *cyclo*-(L-prolyl-L-isoleucyl) ($[\alpha]^{20}_D$ -197°, c = 0.13 (EtOH)) (Adamczeski, Reed, and Crews, 1995). It is known that optical rotations of proline-containing diketopiperazines depended on the configuration of proline; diketopiperazines containing D-proline exhibit positive, whereas those with L-proline show negative (Adamczeski, Reed, and Crews, 1995). Compound F017

had $[\alpha]^{25}_D$ +25.8°, c = 0.14 (MeOH) therefore, it was proposed as *cyclo*-(D-prolyl-isoleucyl), a new derivative of diketopiperazines.

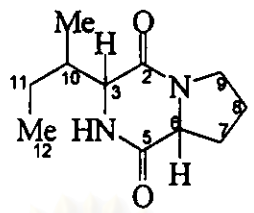

Figure 12. *Cyclo*-(D-prolyl-isoleucyl) (F017) : H-6 = β-H

Cyclo-(L-prolyl-L-isoleucyl) : H-3 and H-6 = α-H

Table 15. ^{1}H and ^{13}C NMR spectral data of *cyclo*-(D-prolyl-isoleucyl) (F017) and *cyclo*-(L-prolyl-L-isoleucyl) (in $CDCl_3$)

Position	F017[a]		*Cyclo*-(L-prolyl-L-isoleucyl)[b]	
	δ_C (ppm)	δ_H (ppm), mult. (*J* in Hz)	δ_C (ppm)	δ_H (ppm), mult. (*J* in Hz)
2	169.3	-	169.9	-
3	62.9	3.74, br s	60.6	3.96, br s
4	-	6.44, NH, br s	-	5.99, brs
5	165.0	-	165.1	-
6	58.4	4.03, br t (7.9)	58.9	4.07, t (7.5)
7a	29.5	1.83, m	28.6	2.0-2.1, m
7b		2.40, m		2.2-2.3, m
8a	22.1	2.35, m	22.4	1.8-1.9, m
8b		2.45		1.9-2.0, m
9a	45.8	3.46, dt (2.4, 10.2)	45.2	3.5-3.6, 2H, m
9b		3.64, m		

Table 15. (continued)

Position	F017[a]		*Cyclo*-(L-prolyl-L-isoleucyl)[b]	
	δ_C(ppm)	δ_H(ppm), mult. (*J* in Hz)	δ_C(ppm)	δ_H(ppm), mult. (*J* in Hz)
10	39.7	2.40, m	35.3	2.3-2.4, m
10-Me	15.4	0.95, 3H, d (6.9)	16.0	1.05, 3H, d (7.2)
11a	24.6	1.20, m	24.1	1.1-1.3, m
11b		1.49, m		1.4-1.5, m
12	11.4	0.88, 3H, t (7.3)	12.2	0.92, 3H, t (7.4)

[a]Data were recorded at 300 MHz (^{1}H) and 75 MHz (^{13}C).
[b]*Cyclo*-(L-prolyl-L-isoleucyl) from Adamczeski, Reed, and Crews, 1995.

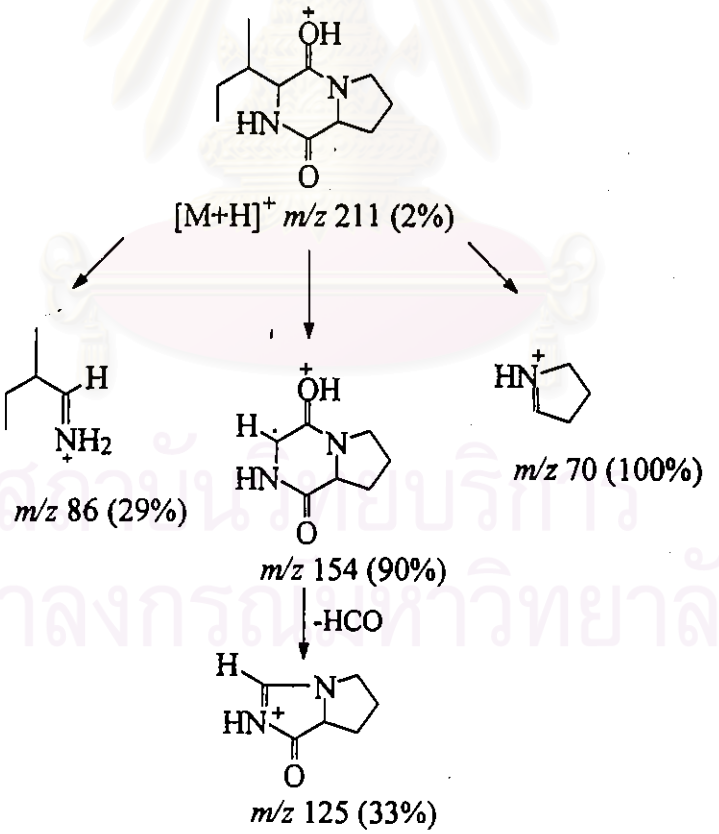

Scheme 7. Proposed mass fragmentation of *cyclo*-(D-prolyl-isoleucyl) (F017)

2.4 *Cyclo*-(D-prolyl-L-phenylalanyl) (P348)

Compound P348 gave a protonated molecular ion $(M+H)^+$ in the HRFABMS (Figure 67) at *m/z* 245.1302 (calculated for *m/z* 245.1290) appropriate for a molecular formula of $C_{14}H_{16}N_2O_2$. The UV spectrum (Figure 68) showed λ_{max} (log ϵ) at 210 (4.15) nm. The IR spectrum (Figure 69) exhibited the maximum absorption bands at 3238 cm^{-1} (amide NH streching), 2926 cm^{-1} (cycloalkane streching), and 1665 cm^{-1} (carbonyl streching).

As seen on the 300 MHz ^1H NMR (in $CDCl_3$) of compound P348 (Figure 70), this compound contained seven methylene proton signals (δ 1.66, 1.78, 1.88, 2.13, 3.06, 3.34, 3.57 ppm), two methine proton signals (δ 2.94, 4.16 ppm), five aromatic methine proton signals (δ 7.14, 7.26 ppm), and one amide proton signal (δ 6.18 ppm). The 75 MHz ^{13}C NMR spectrum (in $CDCl_3$) of compound P348 (Figure 71) showed fourteen carbon signals which could be classified by the DEPT 135 spectrum (Figure 72). Compound P348 showed four methylene carbons (δ 21.8, 29.0, 40.6, 45.2 ppm), two methine carbons (δ 57.8, 59.1 ppm), two amide carbonyl carbons (δ 164.6, 168.9 ppm), and a monosubstituted benzene ring as two sets of two equivalent aromatic methine carbons (δ 128.6, 129.7 ppm), one aromatic methine carbon (δ 127.4 ppm), and one quaternary carbon (δ 135.1 ppm). The HMQC (Figure 73) experiment allowed the assignment of protons attached to carbons (Table 16).

The complete carbon assignment of compound P348 was achieved by analysis of the ^1H-^1H COSY (Figure 74) and HMBC ($^nJ_{HC}$ = 8 Hz) (Figure 75) spectra. The proton correlations in the COSY spectrum (H-3 (δ 4.16 ppm) to 2H-10 (δ 3.06 ppm), NH-4 (δ 6.18

ppm) to H-3 (δ 4.16 ppm) and the proton-carbon long-range correlations in the HMBC spectra (2H-10 (δ 3.06 ppm) to C-3 (δ 59.1 ppm), C-11 (δ 135.1 ppm) and C-12 (δ 129.7 ppm); 2H-10 (δ 3.06 ppm) and NH (δ 6.18 ppm) to C-2 (δ 164.6 ppm)) established the phenylalanine subunit. Similarly, the proton correlations H-6 (δ 2.94 ppm) to 2H-7 (δ 1.78, 2.13 ppm), 2H-7 (δ 1.78, 2.13 ppm) to 2H-8 (δ 1.66, 1.88 ppm), 2H-8 (δ 1.66, 1.88 ppm) to 2H-9 (δ 3.34, 3.57 ppm)) and the proton-carbon long-range correlations (H-6 (δ 2.94 ppm) to C-5 (δ 168.9 ppm) and C-7 (δ 29.0 ppm), H_a-7 (δ 1.78 ppm) to C-5 (δ 168.9 ppm), 2H-7 (δ 1.78, 2.13 ppm) to C-6 (δ 57.8 ppm) and C-8 (δ 21.8 ppm); and 2H-8 (δ 1.66, 1.88 ppm) to C-9 (δ 45.2 ppm)) revealed the proline subunit. The two units were connected by observing the proton-carbon long-range correlations H-3 (δ 4.16 ppm) to C-5 (δ 168.9 ppm) in the HMBC spectrum. Therefore, compound P348 was assigned as a diketopiperazine, *cyclo*-(prolyl-phenylalanyl).

The ^{1}H and ^{13}C NMR spectral data of the compound P348 (Table 16) showed some similarity to that of three known compounds; *cyclo*-(L-prolyl-L-phenylalanyl) isolated from the Antartic sponge-associated bacterium, *Pseudomonas aeruginosa* (Jayatilake *et al.*, 1996); *cyclo*-(L-prolyl-L-phenylalanyl) and *cyclo*-(L-prolyl-D-phenylalanyl) isolated from the pathogenic fungus, *Alternaria alternata* (Stierle, Cardellina, and Strobel, 1988); and *cyclo*-(D-prolyl-D-phenylalanyl) isolated from the Caribbean sponge, *Calyx* cf. *podatypa* (Adamczeski, Reed, and Crews, 1995).

The upfield shift of H-6 (δ 2.94 ppm) suggested that H-6 may be in the same plane of the aromatic ring of the phenylalanine, therefore causing an anisotropy effect.

Previous studies on series of proline-containing diketopiperazines revealed that a folded conformation can be attained in which the aromatic ring is folded over the diketopiperazine ring with the two rings nearly parallel and making van der Waals contacts (Madison, Young, and Blout, 1976). The *cyclo*-(L-prolyl-D-phenylalanyl), in both polar and nonpolar solvents, assume a common folded form (Madison, Young, and Blout, 1976). The upfield shifts of the protons on a diketopiperazine ring in the folded form are the effect of magnetic anisotropy of an aromatic side chain (Westley *et al.*, 1968). In 1995 Adamczeski and coworkers had isolated *cyclo*-(D-prolyl-D-phenylalanyl) and this compound showed $[\alpha]^{20}_{D}$ +68°, c = 0.45 (EtOH) while compound P348 exhibited $[\alpha]^{20}_{D}$ +74.52°, c = 0.37 (MeOH). The positive optical rotation indicated the D-prolyl in compound P348 (Adamczeski, Reed, and Crews, 1995). However, H-6 of *cyclo*-(D-prolyl-D-phenylalanyl) and compound P348 resonanced differently (δ 4.08 ppm for *cyclo*-(D-prolyl-D-phenylalanyl) and δ 2.94 ppm for compound P348), so compound P348 was not *cyclo*-(D-prolyl-D-phenylalanyl). To prove the fact that the upfield shift of H-6 is present in DL or LD in the molecule of *cyclo*-(prolyl-phenylalanyl), chemical synthesis of *cyclo*-(L-prolyl-L-phenylalanyl) has been carried out, employing the method of Bodanszky, M. and Bodanszky, A., 1994. The synthetic *cyclo*-(L-prolyl-L-phenylalanyl) in Section 2.4.1 showed proton signals of H-3 and H-6 at δ 4.25, 4.06 ppm, respectively. The upfield shift of H-6 and the positive optical rotation for compound P348 suggested that this compound should be a new *cyclo*-(D-prolyl-L-phenylalanyl).

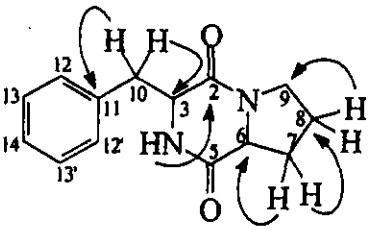

Figure 13. The long-range correlations in the HMBC spectrum of *cyclo*-(D-prolyl-L-phenylalanyl) (P348)

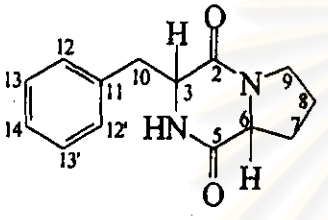

Figure 14. *Cyclo*-(prolyl-phenylalanyl)

Compounds	H-3	H-6
cyclo-(L-prolyl-L-phenylalanyl)	α	β
cyclo-(D-prolyl-L-phenylalanyl	β	α
cyclo-(L-prolyl-D-phenylalanyl)	α	β
cyclo-(D-prolyl-D-phenylalanyl	β	β

Table 16. ^{1}H and ^{13}C NMR spectral data of *cyclo*-(D-prolyl-L-phenylalanyl) (P348), *cyclo*-(L-prolyl-L-phenylalanyl), *cyclo*-(L-prolyl-D-phenylalanyl), and *cyclo*-(D-prolyl-D-phenylalanyl), (in $CDCl_3$)

Position	*Cyclo*-(D-prolyl-L-phenylalanyl) (P348)[a]		*Cyclo*-(L-prolyl-L-phenylalanyl) (dkp 27)[a]		*Cyclo*-(L-prolyl-L-phenylalanyl)[b]	*Cyclo*-(L-prolyl-D-phenylalanyl)[b]	*Cyclo*-(D-prolyl-D-phenylalanyl)[c]	
	δ_C (ppm)	δ_H (ppm), mult. (*J* in Hz)	δ_C (ppm)	δ_H (ppm), mult. (*J* in Hz)	δ_H (ppm), mult. (*J* in Hz)	δ_H (ppm), mult. (*J* in Hz)	δ_C (ppm)	δ_H (ppm), mult. (*J* in Hz)
2	164.6	-	164.8	-	-	-	ND	-
3	59.1	4.16, dd (4.1, 10.1)	56.2	4.25, dd (3.0, 9.9)	4.20, dd (3.2, 10.3)	4.20, dd (3.3, 10.3)	56.2	4.27, dd (2.6, 10.6)
4	-	6.18, NH, br s	-	5.64, NH, br s	5.70, NH, s	6.20, NH, s	-	5.60, NH, br s
5	168.9	-	169.1	-	-	-	ND	-
6	57.8	2.94, dd (6.6, 10.0)	59.2	4.06, dd (7.4)	4.07, t (7.1)	3.38, m	59.2	4.08, t (7.1)

Table 16. (continued)

Position	*Cyclo*-(D-prolyl-L-phenylalanyl) (P348)[a]		*Cyclo*-(L-prolyl-L-phenylalanyl) (dkp 27)[a]		*Cyclo*-(L-prolyl-L-phenylalanyl)[b]	*Cyclo*-(L-prolyl-D-phenylalanyl)[b]	*Cyclo*-(D-prolyl-D-phenylalanyl)[c]	
	δ_C (ppm)	δ_H (ppm), mult. (*J* in Hz)	δ_C (ppm)	δ_H (ppm), mult. (*J* in Hz)	δ_H (ppm), mult. (*J* in Hz)	δ_H (ppm), mult. (*J* in Hz)	δ_C (ppm)	δ_H (ppm), mult. (*J* in Hz)
7a	29.0	1.78, m	28.5	2.00, m	1.93, m	1.80, m	28.4	2.0-2.1, m
7b		2.13, dd (6.0, 12.2)		2.32, m	2.31, m	2.21, m		2.3-2.4, m
8a	21.8	1.66, m	22.7	1.98, 2H, m	1.93, 2H, m	1.80, 2H, m	22.6	1.8-1.9, 2H, m
8b		1.88, m						
9a	45.2	3.34, m	45.5	3.57, 2H, m	3.59, 2H, m	3.08, 2H, m	45.6	3.5-3.6, m
9b		3.57, m						3.6-3.7, m
10a	40.6	3.06, 2H, m	36.9	2.76, dd (9.9, 14.3)	2.76, dd (10.3, 15.1)	3.01, t (7.4)	36.9	2.77, dd (10.8, 14.4)
10b				3.60, dd (14.3, 3.0)	3.64, dd, (3.2, 15.1)	3.38, m		3.5-3.6, m
11	135.1	-	135.8	-	-	-	129.4	-
12, 12'	129.7[d] 129.7[d]		129.2[d] 129.2[d]				129.2[d] 129.2[d]	
13, 13'	128.6[d] 128.6[d]	7.14-7.26, 5H, m	129.0[d] 129.0[d]	7.19-7.35, 5H, m	7.22, 5H, br s	7.22, 5H, br s	127.6[d] 127.6[d]	7.2-7.4, 5H
14	127.4		127.4[d]				129.6	

[a]Data were recorded at 300 MHz (^{1}H) and 75 MHz (^{13}C).
[b]*Cyclo*-(L-prolyl-L-phenylalanyl) and *cyclo*-(L-prolyl-D-phenylalanyl) from Stierle, Cardellina, and Strobel, 1988.
[c]*Cyclo*-(D-prolyl-D-phenylalanyl) from Adamczeski, Reed, and Crews, 1995.
[d]Assignments may be interchangeable.

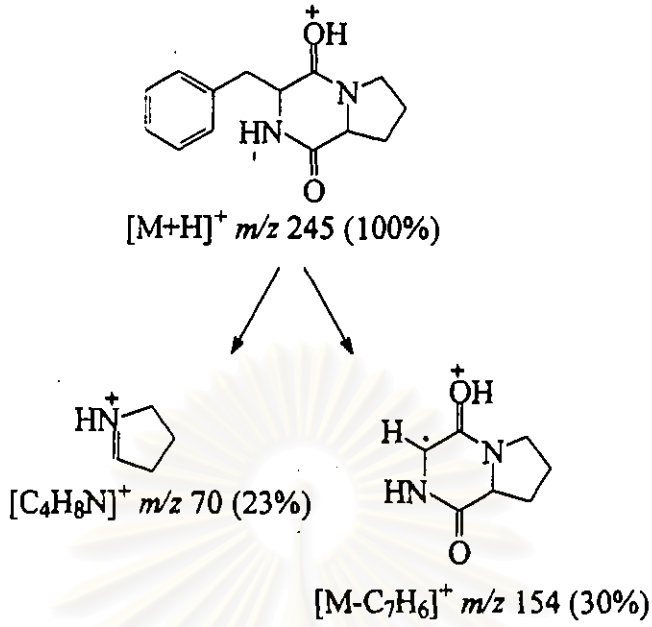

Scheme 8. Proposed mass fragmentation of *cyclo*-(D-prolyl-L-phenylalanyl) (P348)

2.4.1 Synthetic *cyclo*-(L-prolyl-L-phenylalanyl) (dkp27)

Cyclo-(L-prolyl-L-phenylalanine) was synthesized from L-proline and L-phenylalanine according to the method of Bodanszky, A. and Bodanszky, M., 1994 (Experimental section 11). The crude *cyclo*-(L-prolyl-L-phenylalanine) was purified by silica gel flash chromatography to yield a compound dkp27.

The MS, UV, IR, and NMR spectra of compound dkp27 (Figures 76-84 and Table 16) were very similar to those of compound P348 suggesting that the two molecules were closely related. Differences in the ^{1}H NMR spectrum (in $CDCl_3$) of compound dkp27 (Figure 79) compared to that of compound P348 (Figure 70) were H-6 of compound dkp27 was downfield to δ 4.06 ppm, while that of compound P348 was upfield to δ 2.94 ppm. The major difference in the optical rotations for the two compounds was the

negative optical rotation ($[\alpha]^{25}_{D}$ -39.10°, c = 0.14 (MeOH)) for compound dkp27 and the positive optical rotation ($[\alpha]^{25}_{D}$ +74.52°, c = 0.37 (MeOH)) for compound P348. It can be confirmed that compound dkp27 should be *cyclo*-(L-prolyl-L-phenylalanyl), while compound P348 was *cyclo*-(D-prolyl-L-phenylalanyl).

2.5 *Cyclo*-(*trans*-4-hydroxy-L-prolyl-L-phenylalanyl) (F018)

The electron impact mass spectrum of compound F018 (Figure 85) showed the molecular ion peak at *m/z* 260 $(M)^+$ implying a molecular formula of $C_{14}H_{16}N_2O_3$. The UV spectrum (Figure 86) exhibited λ_{max} (log ϵ) at 206 (4.45) nm, and the IR spectrum (Figure 87) exhibited the maximum absorption bands at 3382 cm^{-1} (OH streching), 3004 cm^{-1} (amide NH streching), 2457 cm^{-1} (cycloalkane streching), 1681 cm^{-1} (carbonyl streching), and 1455 cm^{-1} (aromatic ring streching).

Generally, the ^1H (Figures 88 and 89) and ^{13}C (Figure 90) NMR spectra (in $CDCl_3$) of compound F018 were similar to those of compound P348. The ^{13}C NMR (Figure 90) and DEPT 135 (Figure 91) spectral data of compound F018 revealed that a methylene carbon at C-8 (δ 21.8 ppm) of compound P348 was replaced a hydroxyl methine carbon at δ 68.2 ppm of compound F018. Extensive NMR data analysis using HETCOR (Figure 92), ^1H-^1H COSY (Figure 93), TOCSY (Figure 94), and HMBC (Figure 95) techniques, led to the identification of F018 as *cyclo*-(4-hydroxy-prolyl-phenylalanyl). The results obtained from the HMBC (Figure 95) spectral data revealed correlations of 2H-10 (δ 2.75, 3.51 ppm) to C-2 (δ 164.9 ppm), C-3 (δ 56.2 ppm) and C-11 (δ 135.5 ppm) leading to the assignment of C-2 (δ

164.9 ppm) and C-5(δ 169.6 ppm). The complete assignment of protons and carbons in F018 is in Table 17.

H-6 of compound F018 resonated at δ 4.38 ppm (Figures 88 and 89), while that of compound P348 appeared more upfield at δ 2.94 ppm (Figure 70), suggesting the different orientation of an aromatic ring of phenylalanine moiety on compounds F018 and P348. The *cis* orientation of H-3 and H-6, and the *trans* orientation of H-6 and H-8 were determined by the NOESY spectrum of compound F018 (Figure 96), so compound F018 could be either *cyclo*-(*trans*-4-hydroxy-L-prolyl-L-phenylalanyl) or *cyclo*-(*trans*-4-hydroxy-D-prolyl-D-phenylalanyl). Optical rotation of compound F018 ($[\alpha]^{25}_{D}$ –77.5°, c = 0.14 (MeOH)) was negative while that of known *cyclo*-(*trans*-4-hydroxy-L-prolyl-L-phenylalanyl) ($[\alpha]^{25}_{D}$–6.7°, c = 0.016 (MeOH)) was also negative (Adamczeski, Quinoa, and Crews, 1989). The ^{1}H and ^{13}C NMR spectral data of compound F018 (Table 17) were similar to *cyclo*-(*trans*-4-hydroxy-L-prolyl-L-phenylalanyl) previously isolated from the unidentified Jaspidae sponge (Adamczeski, Quinoa, and Crews, 1989). Compound F018 was therefore *cyclo*-(*trans*-4-hydroxy-L-prolyl-L-phenylalanyl).

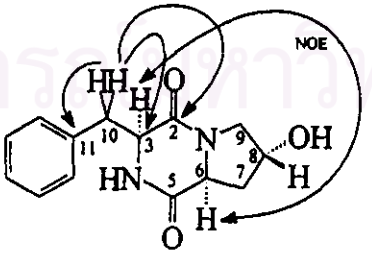

Figure 15. The long-range correlations (→) and the NOESY correlations (↔) of *cyclo*-(*trans*-4-hydroxy-L-prolyl-L-phenylalanyl) (F018)

Table 17. ^{1}H and ^{13}C NMR spectral data of *cyclo*-(*trans*-4-hydroxy-L-prolyl-L-phenylalanyl) (F018) (in $CDCl_3$) and *cyclo*-(*trans*-4-hydroxy-L-prolyl-L-phenylalanyl) (in $CDCl_3$)

Position	*Cyclo*-(*trans*-4-hydroxy-L-prolyl-L-phenylalanyl).(F018)[a]		*Cyclo*-(*trans*-4-hydroxy-L-prolyl-L-phenylalanyl)[b]	
	δ_C (ppm)	δ_H (ppm), mult. (*J* in Hz)	δ_C (ppm)	δ_H (ppm), mult. (*J* in Hz)
2	164.9	-	169.8	-
3	56.2	4.25, br d (10.9)	56.2	4.31, dd (2.6, 10.7)
4	-	5.87, NH, br s	-	5.89, NH, s
5	169.6	-	166.2	-
6	57.4	4.38, dd (5.9, 10.7)	57.4	4.47, dd (6.3, 11.1)
7a	37.7	1.86, br dd (10.7, 13.2)	37.7	2.06, ddd (4.2, 11.4, 13.5)
7b		2.27, br dd (5.9, 13.2)		2.36, dd (6.2, 13.2)
8	68.2	4.47, br s	68.2	4.60, t (4.1)
9a	54.5	3.48, br d (13.1)	54.4	3.58, d (13.8)
9b		3.69, dd (3.9, 13.1)		3.80, dd (4.5, 13.2)
10a	36.7	2.75, dd (10.9, 14.3)	36.7	2.77, dd (10.9, 14.6)
11b		3.51, br d (14.3)		3.63, dd (3.9, 15.9)
11	135.5	-	135.8	-
12, 12'	129.1[c]		129.3	
13, 13'	129.0[c]	7.10-7.30, 5H, m	129.2	7.29, m
14	127.4		127.6	

[a]Data were recorded at 300 MHz (^{1}H) and 75 MHz (^{13}C).
[b]*Cyclo*-(*trans*-4-hydroxy-L-prolyl-L-phenylalanyl) from Adamczeski, Quinoa, and Crews, 1989.
[c]Interchangeable.

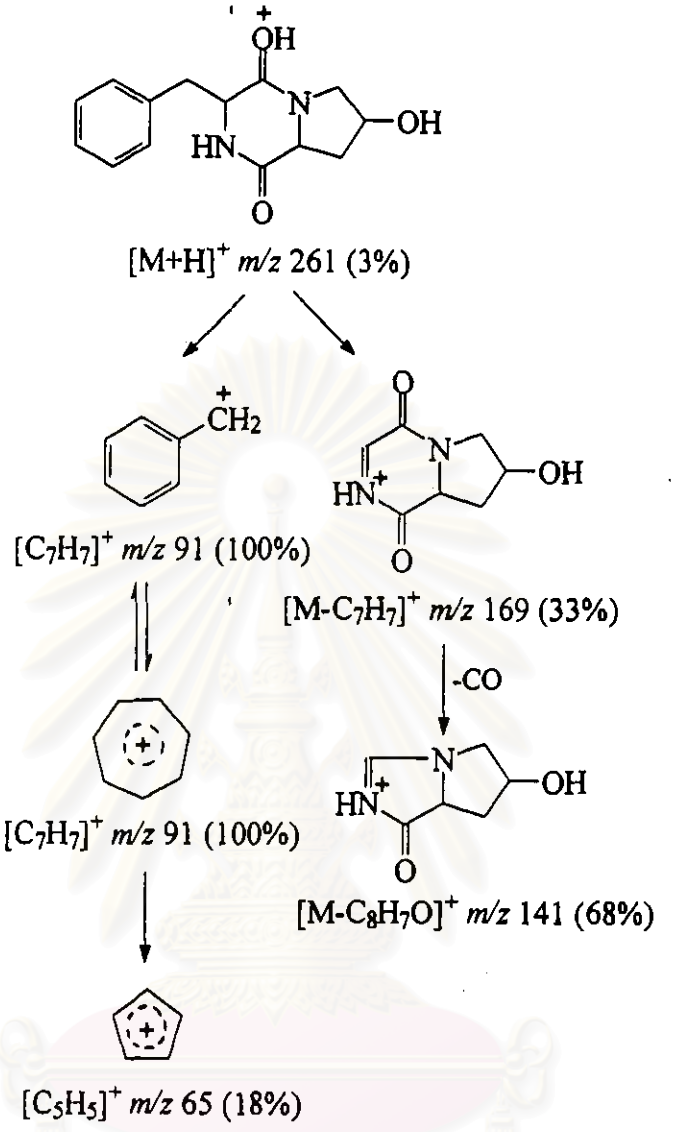

Scheme 9. Proposed mass fragmentation of *cyclo*-(*trans*-4-hydroxy-L-prolyl-L-phenylalanyl) (F018)

สถาบันวิทยบริการ
จุฬาลงกรณ์มหาวิทยาลัย

2.6 *Cyclo*-(L-prolyl-L-tryptophanyl) (P350) and *cyclo*-(D-prolyl-L-tryptophanyl) (P352)

Compounds P350 and P352 (Figures 97 and 98) analyzed for $C_{16}H_{18}N_3O_2$ $(M+H)^+$ by HRFABMS at *m/z* 284.1412 $(M+H)^+$ and 284.1400 $(M+H)^+$, respectively (calculated for *m/z* 284.1399 $(M+H)^+$) and a fragment ion at *m/z* 154 due to the loss of indole side chain of the amino acid tryptophan. The UV and IR spectral data of compounds P350 and P352 are described in Table 18. The IR spectrum of compounds P350 and P352 (Figures 101 and 102) suggested the presence of amide NH (ν_{max} 3278 and 3270 cm^{-1} for compounds P350 and P352, respectively), cycloalkane (ν_{max} 2924 and 2918 cm^{-1} for compounds P350 and P352, respectively), and carbonyl (ν_{max} 1667 and 1651 cm^{-1} for compounds P350 and P352, respectively) groups.

The 400 MHz ^1H NMR spectra (in $CDCl_3$) of compounds P350 and P352 (Figures 103 and 104) are similar except that H-12 (δ 2.83 ppm) of compound P352 shifted upfield, while H-12 (δ 4.07 ppm) of compound P350 was rather downfield. The 75 MHz ^{13}C and DEPT 135 NMR spectra (in $CDCl_3$) of both compounds (Figures 105-108) revealed four methylene carbons, two methine carbons, five aromatic carbons, and five quaternary carbons.

The HMQC (Figures 108 and 109) and ^1H-^1H COSY (Figures 111 and 112) NMR spectra of compounds P350 and P352 allowed the assignment of protons correlated to carbons, while the complete assignment of compounds P350 and P352 was achieved by analysis of the HMBC ($^nJ_{HC}$ = 4 and 8 Hz) NMR spectra (Figures 113-115). The ^1H-^1H COSY NMR spectral data of compounds P350 and P352 showed correlations of H-4 to H-5;

H-5 to H-6; H-6 to H-7; 2H-8 to H-9; H-12 to 2H-17; 2H-17 to 2H-16; and 2H-16 to 2H-15. Both compounds P350 and P352 exhibited the similar ^{1}H-^{13}C correlations as follows: H-2 to C-3, C-3a and C-8; H-4 to C-3a and C-4; H-4 to C-5; H-5 to C-6; H-6 to C-7; H-7 to C-3a; 2H-8 to C-3, C-3a, C-9 and C-14; H-9 to C-8 and C-14; 2H-15 to C-16; 2H-17 to C-12 and C-16. Based on these spectral data, compounds P350 and P352 were a diketopiperazine, *cyclo*-(prolyl-tryptophanyl).

The ^{1}H and ^{13}C NMR spectral data of compounds P350 and P352 (Table 19) were found to be similar to that of the previously isolated compounds (Table 20), brevianamide F (*cyclo*-(L-prolyl-L-tryptophanyl)) from the fungus, *Penicillium brevi-compactum* Dierckx (Birch and Russell, 1972) and the marine bacterium, *Vibrio* sp. (Kobayashi *et al.*, 1994); and formerly synthetic compounds (Table 20), *cyclo*-(L-prolyl-L-tryptophanyl) and *cyclo*-(D-prolyl-L-tryptophanyl) (Sammes *et al.*, 1979).

The differences between compounds P350 and P352 were optical rotations and δ_H of H-12. The relative configuration of two methine protons (H-9 and H-12) of compounds P350 and P352 were demonstrated by the NOESY spectra (Figures 116 and 117). The NOESY spectrum of compound P350 showed the correlation of H-9 and H-12 (Figure 116), whereas that of compound P352 did not exhibit such correlation (Figure 117). The optical rotation of compound P350 ($[\alpha]^{25}_{D}$ -38.5°, c = 0.23 (MeOH)) was found to be similar to those of brevianamide F (*cyclo*-(L-prolyl-L-tryptophanyl)) ($[\alpha]^{25}_{D}$ -64°, c = 0.69 (MeOH)) (Kobayashi *et al.*, 1994) and the synthetic *cyclo*-(L-prolyl-L-tryptophanyl) ($[\alpha]^{25}_{D}$ -99°, c = 1.2 (AcOH)) (Sammes *et al.*, 1979), while the optical rotation of compound P352 ($[\alpha]^{25}_{D}$

+145.4°, c = 0.05 (MeOH)) was found to be similar to that of synthetic *cyclo*-(D-prolyl-L-tryptophanyl) ($[\alpha]^{25}_D$ +120°, c = 1.3 (AcOH)) (Sammes *et al.*, 1979) (Table 18). Furthermore proton chemical shift at H-12 of compound P352 (δ 2.83 ppm) was more upfield than that of compound P350 (δ 4.07 ppm) due to the anisotropy effect of an indole ring of tryptophan. Finally, it was concluded that compounds P350 and P352 were identified as *cyclo*-(L-prolyl-L-tryptophanyl) and *cyclo*-(D-prolyl-L-tryptophanyl), respectively. The discovery of *cyclo*-(D-prolyl-L-tryptophanyl) in *Bacillus* sp. Sc026 was the first report from natural sources.

Table 18. Optical rotations, λ_{max}, ν_{max}, *m/z* of *cyclo*-(L-prolyl-L-tryptophanyl) (P350), *cyclo*-(D-prolyl-L-tryptophanyl) (P352), brevianamide F (*cyclo*-(L-prolyl-L-tryptophanyl)), synthetic *cyclo*-(L-prolyl-L-tryptophanyl), and synthetic *cyclo*-(D-prolyl-L-tryptophanyl)

Compounds	$[\alpha]_D$ (°)	λ_{max} (log∈) (nm)	ν_{max} (cm^{-1})	*m/z* (% relative intensity)
cyclo-(L-prolyl-L-tryptophanyl) (P350)	-38.5 (0.23 in MeOH at 25°C)	280 (3.46), 219 (4.23)	3278, 2924, 1667, 1434	284 (64), 154 (88), 130 (100), 107 (23), 89 (20), 77 (18)
cyclo-(D-prolyl-L-tryptophanyl) (P352)	+145.4 (0.05 in MeOH at 25°C)	279 (3.82), 220 (4.57)	3270, 2918, 1651, 1455	284 (27), 154 (100), 136 (68), 107 (21), 89 (18), 77 (16)
brevianamide F (*cyclo*-(L-prolyl-L-tryptophanyl))[a]	ND	292, 283, 277	3280, 1670, 1650, 1640	283 (9), 154 (8), 130 (100), 83 (9)

Table 17. (continued)

Compounds	$[\alpha]_D$ (°)	λ_{max} (log∈) (nm)	ν_{max} (cm^{-1})	*m/z* (% relative intensity)
brevianamide F (*cyclo*-(L-prolyl-L-tryptophanyl))[b]	-64 (0.69 in MeOH at 25°C)	290 (3.2), 281 (3.3), 276 (3.3), 220 (4.0)	3264, 1694, 1265	ND
synthetic *cyclo*-(L-prolyl-L-tryptophanyl)[c]	-99 (1.2 in AcOH at 24°C)	ND	ND	ND
synthetic *cyclo*-(D-prolyl-L-tryptophanyl)[c]	+120 (1.3 in AcOH at 20°C)	289 (3.6), 279 (3.7), 273 (3.7), 220 (4.4)	ND	ND

[a]Brevianamide F (*cyclo*-(L-prolyl-L-tryptophanyl)) from Birch and Russell, 1972.
[b]Brevianamide F (*cyclo*-(L-prolyl-L-tryptophanyl)) from Kobayashi *et al.*, 1994.
[c]Synthetic *cyclo*-(L-prolyl-L-tryptophanyl) and synthetic *cyclo*-(D-prolyl-L-tryptophanyl from Sammes *et al.*, 1979.
ND = No data.

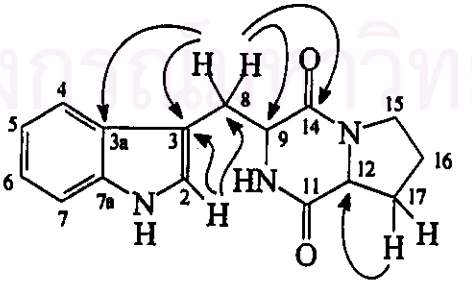

Figure 16. The long-range correlations in the HMBC spectra of *cyclo*-(L-prolyl-L-tryptophanyl) (P350) and *cyclo*-(D-prolyl-L-tryptophanyl) (P352)

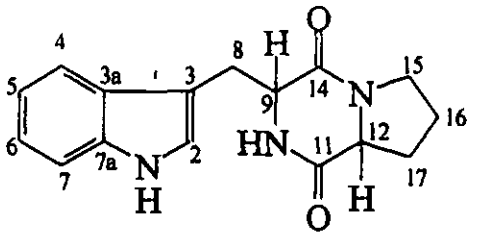

Figure 17. *Cyclo*-(prolyl-tryptophanyl)

cyclo-(L-prolyl-L-tryptophanyl) : H-9 and H-12 = α-H

cyclo-(D-prolyl-L-tryptophanyl) : H-9 = α-H, H-12 = β-H

Table 19. ^{1}H and ^{13}C NMR spectral data of *cyclo*-(L-prolyl-L-tryptophanyl) (P350) and *cyclo*-(D-prolyl-L-tryptophanyl) (P352) (in $CDCl_3$)

Position	*Cyclo*-(L-prolyl-L-tryptophanyl) (P350)[a]		*Cyclo*-(D-prolyl-L-tryptophanyl) (P352)[a]	
	δ_C (ppm)	δ_H (ppm), mult. (*J* in Hz)	δ_C (ppm)	δ_H (ppm), mult. (*J* in Hz)
1	-	7.19, NH, br s	-	8.16, NH, br s
2	123.2	7.12, d (1.7)	124.0	7.06, d (2.1)
3	109.9	-	109.4	-
3a	126.6	-	126.8	-
4	118.4	7.58, d (7.6)	118.8	7.60, d (7.6)
5	122.7	7.22, dd (7.6, 7.6)	122.5	7.17, dd (7.6, 7.6)
6	119.9	7.25, dd (7.6, 7.6)	119.8	7.12, dd (7.6, 7.6)
7	111.5	7.35, d (7.6)	111.1	7.35, d (6.4)
7a	136.5	-	136.0	-

Table 19. (continued)

Position	*Cyclo*-(L-prolyl-L-tryptophanyl) (P350)[a]		*Cyclo*-(D-prolyl-L-tryptophanyl) (P352)[a]	
	δ_C (ppm)	δ_H (ppm), mult. (*J* in Hz)	δ_C (ppm)	δ_H (ppm), mult. (*J* in Hz)
8a	27.0	2.96, dd (10.8, 15.2)	30.8	3.18, dd (3.8, 14.9)
8b		3.75, dd (3.2, 15.2)		3.40, dd (6.2, 14.6)
9	54.6	4.36, dd (3.2, 10.8)	58.5	4.24, dd (3.8, 6.2)
10	-	5.75, NH, br s	-	6.00, NH, br s
11	169.1	-	169.2	-
12	59.3	4.07, t (7.7)	57.9	2.83, dd (6.5, 10.9)
14	165.3	-	165.1	-
15a	45.5	3.54-3.68, 2H, m	45.2	3.16, dd (3.1, 9.6)
15b				3.54,m
16a	22.7	1.84-2.07, 2H, m	21.7	1.43, m
16b				1.83, m
17a	28.4	2.01, m	29.1	1.72, m
17b		2.31, m		2.07, m

[a]Data were recorded at 400 MHz (^{1}H) and 75 MHz (^{13}C).

สถาบันวิทยบริการ
จุฬาลงกรณ์มหาวิทยาลัย

Table 20. ^{1}H and ^{13}C NMR spectral data of brevianamide F (*cyclo*-(L-prolyl-L-tryptophanyl), and synthetic *cyclo*-(D-prolyl-L-tryptophanyl)

Position	brevianamide F (*cyclo*-(L-prolyl-L-tryptophanyl))[a] (in $CDCl_3$)		brevianamide F (*cyclo*-(L-prolyl-L-tryptophanyl))[b] (in DMSO-d_6)	synthetic *cyclo*-(D-prolyl-L-tryptophanyl)[c] (in $CDCl_3$)
	δ_C (ppm)	δ_H (ppm), mult. (*J* in Hz)	δ_H (ppm), mult. (*J* in Hz)	δ_H (ppm), mult. (*J* in Hz)
1	-	8.30, NH, br s	10.8, NH	8.50, NH, br s
2	123.3	7.1-7.2, m	7.98, d (2)	6.80, s
3	109.9	-	-	-
3a	126.7	-	-	-
4	118.5	7.39, d-like (8)		
5	122.7	7.1-7.2, 2H, m		
6	120.0		6.9-7.6, 4H, m	6.90-7.60, 4H, m
7	111.5	7.59, d-like (8)		
7a	136.6	-	-	-
8a	26.8	2.97, dd (11, 15)	2.9-3.5, 2H, m	2.60, m
8b		3.76, dd (3.5, 15)		2.78-3.60, m
9	54.5	4.38, dd (3.5, 11)	4.05, t (7)	4.16, br s (after D_2O exchange)
10	-	5.74, NH, br s	7.66, NH	6.90-7.60, NH
11	169.3	-	-	-
12	59.2	4.08, t-like (7.5)	4.30, t (6)	2.78-3.60, m[d]

สถาบันวิทยบริการ
จุฬาลงกรณ์มหาวิทยาลัย

Table 20. (continued)

Position	brevianamide F (*cyclo*-(L-prolyl-L-tryptophanyl))[a] (in $CDCl_3$)		brevianamide F (*cyclo*-(L-prolyl-L-tryptophanyl))[b] (in DMSO-d_6)	synthetic *cyclo*-(D-prolyl-L-tryptophanyl)[c] (in $CDCl_3$)
	δ_C (ppm)	δ_H (ppm), mult. (*J* in Hz)	δ_H (ppm), mult. (*J* in Hz)	δ_H (ppm), mult. (*J* in Hz)
14	165.4	-	-	-
15	45.4	3.64, 2H, m	2.9-3.5, 2H, m	2.78-3.60, 2H, m[d]
16	22.6	2.0-2.3, 4H, m	1.2-2.1, 4H, m	1.10-2.10, 4H, m
17	28.3			

[a]Brevianamide F (*cyclo*-(L-prolyl-L-tryptophanyl)) from Kobayashi *et al.*, 1994.
[b]Brevianamide F (*cyclo*-(L-prolyl-L-tryptophanyl)) from Birch and Russell, 1972.
[c]Synthetic *cyclo*-(D-prolyl-L-tryptophanyl) from Sammes *et al.*, 1979.
[d]Overlapping signals.

สถาบันวิทยบริการ
จุฬาลงกรณ์มหาวิทยาลัย

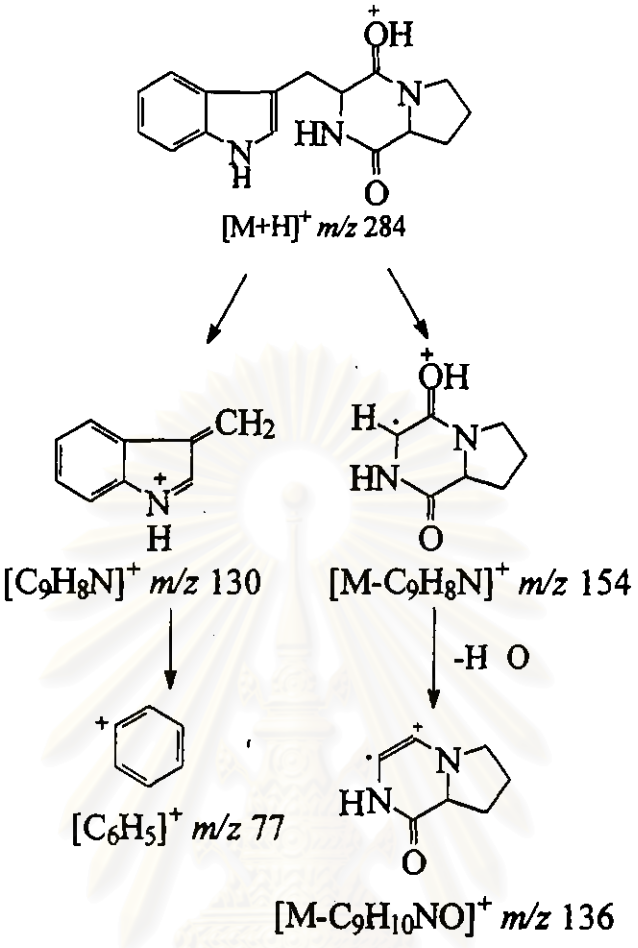

Scheme 10. Proposed mass fragmentation of *cyclo*-(L-prolyl-L-tryptophanyl) (P350) and *cyclo*-(D-prolyl-L-tryptophanyl) (P352)

สถาบันวิทยบริการ
จุฬาลงกรณ์มหาวิทยาลัย

2.7 2'Deoxyadenosine (S147)

The FABMS of compound S147 (Figure 116) gave the protonated molecular ion peak at *m/z* 252 $(M+H)^+$ indicative of a molecular formula of $C_{10}H_{13}N_5O_3$. Proposed mass fragmentation of compound S147 was shown in Scheme 11. The UV spectrum (Figure 117) showed λ_{max} (log ϵ) at 210 (4.06) and 260 (3.92) nm. The IR spectrum (Figure 118) indicated the presence of two hydroxyl groups at 3342 cm^{-1}, an primary amine group at 3210 cm^{-1}, and an aromatic C-C at 1609 cm^{-1}.

The 300 MHz ^1H NMR spectrum (in DMSO-d_6) of compound S147 (Figure 119), showed four methylene proton signals (δ 2.25, 2.71, 3.51, 3.61 ppm), three methine proton signals (δ 3.87, 4.39, 6.33 ppm), two olefinic proton (δ 8.10, 8.32 ppm), one amine proton signal (δ 7.28 ppm), and two hydroxyl proton signals (δ 5.25, 5.32 ppm). The 75 MHz ^{13}C NMR spectrum (in DMSO-d_6) of compound S147 (Figure 120) exhibited ten carbon signals which could be classified by DEPT 135 spectrum (Figure 121) as two methylene carbons (δ 38.7, 62.0 ppm), three methine carbons (δ 71.1, 84.0, 88.1 ppm), two olefinic carbons (δ 139.5, 152.3 ppm), three quaternary carbons (δ 119.3, 148.8, 156.0 ppm). Compound S147 showed optical rotation ($[\alpha]^{25}_D$ –7.6°, c = 0.50 (MeOH)).

The complete assignments of compound S147 were achieved by the analysis of the HMQC, ^1H-^1H COSY, and HMBC spectra (Figures 124-127). The ^1H-^1H COSY spectrum of compound S147 (Figure 123) demonstrated the correlations of H-1' (δ 6.33 ppm) to 2H-2' (δ 2.25, 2.71 ppm); 2H-2' (δ 2.25, 2.71 ppm) to H-3' (δ 4.39 ppm); H-3' (δ 4.39 ppm) to H-4' (δ 3.87 ppm); H-4' (δ 3.87 ppm) to 2H-5' (δ 3.51, 3.61 ppm); 2H-5' (δ 3.51, 3.61 ppm) to OH-5' (δ 5.25 ppm); and H-3' (δ 4.39 ppm) to OH-3' (δ 5.32

ppm). According to the HMBC ($^{n}J_{HC}$ = 4 and 8 Hz) spectra of compound S147 (Figures 123 and 124), two quaternary carbon signals at δ 148.8 and 119.3 ppm were assigned as C-4 and C-5, respectively, by the long-range coupling with H-2 (δ 8.10 ppm) and H-8 (δ 8.32 ppm). The quaternary carbon signal and the aromatic methine carbon signals at δ 148.8 and 139.5 ppm were assigned as C-4 and C-8, respectively, by the long-range coupling with H-1' (δ 6.33 ppm). Compound S147 was then proposed as the known purine nucleoside, 2'-deoxyadenosine previously isolated from the sponge *Dasychalina cyathina* (Weinheimer *et al.*, 1978).

The ^{1}H and ^{13}C NMR spectral data of 2'-deoxyadenosine didn't show in the previous report (Weinheimer *et al.*, 1978). Herein, the proton chemical shifts of 2'-deoxyadenosine (S147) and the comparison of carbon chemical shifts between 2'-deoxyadenosine (S147) and adenosine (Pretsch *et al.*, 1983) were shown in Table 21. The ^{13}C NMR spectral data of 2'-deoxyadenosine (S147) (Table 21) was found to be similar to that of adenosine (Pretsch *et al.*, 1983) except for the carbon chemical shift at C-2. 2'-Deoxyadenosine (S147) exhibited methylene carbon (C-2) at δ 38.7 ppm, while adenosine showed methine carbon with hydroxy group at δ 73.8 ppm.

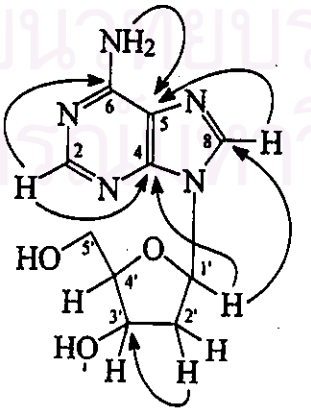

Figure 18. The long-range correlations in the HMBC spectrum of 2'deoxyadenosine (S147)

Table 21. ^{1}H and ^{13}C NMR spectral data of 2'-deoxyadenosine (S147) and adenosine (in DMSO-d_6)

Position	2'-Deoxyadenosine (S147)[a]		Adenosine[b]
	δ_C (ppm)	δ_H (ppm), mult. (*J* in Hz)	δ_C (ppm)
2	152.3	8.10, br s	152.6
4	148.8	-	149.3
5	119.3	-	119.6
6	156.0	-	156.3
6-NH_2	-	7.28, 2H, br s	-
8	139.5	8.32, br s	140.2
1'	84.0	6.33, t (6.6)	88.2
2'	38.7	2.25, m 2.71, m	73.8
3'	71.1	4.39, d (2.3)	70.9
4'	88.1	3.87, d (2.3)	86.2
5'	62.0	3.51, m 3.61, m	61.9
3'-OH	-	5.32, d (3.8)	-
5'-OH	-	5.25, t (5.6)	-

[a]Data were recorded at 300 MHz (^{1}H) and 75 MHz (^{13}C).
[b]Adenosine from Pretsch *et al.*, 1983.

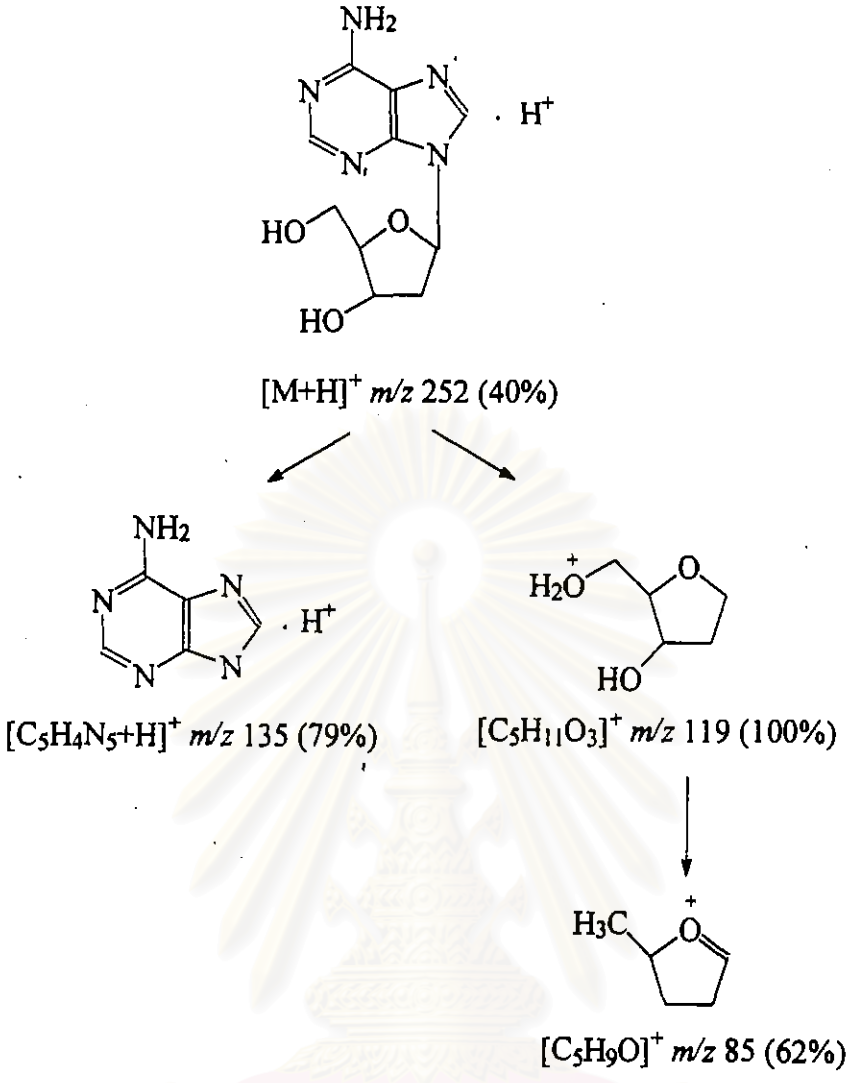

Scheme 11. Proposed mass fragmentation of 2'deoxyadenosine (S147)

สถาบันวิทยบริการ
จุฬาลงกรณ์มหาวิทยาลัย

2.8 Macrolactin F (P035), 7-*O*-succinyl macrolactin F (P129), and 7-*O*-succinyl macrolactin A (P103)

2.8.1 Macrolactin F (P035)

The HRFABMS (Figure 126) established the molecular formula of compound P035 as $C_{24}H_{34}O_5$ by showing the molecular ion peak at *m/z* 425.2326 $(M+Na)^+$ (calculated for $C_{24}H_{34}O_5Na$, 425.2304). The UV spectrum (Figure 129) exhibited λ_{max} (log ϵ) at 235 (4.21) and 261 (4.12) nm. The IR spectrum (Figure 132) suggested the presence of hydroxyl groups (ν_{max} 3415 cm^{-1}), ester carbonyl (ν_{max} 1707 cm^{-1}), and ketone carbonyl moieties (ν_{max} 1638 cm^{-1}).

As seen on the 400 MHz ^1H NMR spectrum (in $CDCl_3$) of compound P035 (Figures 135 and 138), this compound contained one methyl proton signal (δ 1.17 ppm), eleven methylene proton signals (δ 1.38, 1.48, 1.58, 1.90, 1.97, 2.20, 2.39, 2.42, 2.46, 2.53, 2.60 ppm), and thirteen methine proton signals (δ 4.03, 4.29, 4.96, 5.34, 5.35, 5.45, 5.54, 5.72, 5.99, 6.09, 6.43, 6.50, 7.23 ppm). The 100 MHz ^{13}C NMR spectrum (in $CDCl_3$) of compound P035 (Figure 142) showed twenty four carbon signals which could be classified by DEPT 135 spectrum (Figure 145) as one methyl carbon signal (δ 20.0 ppm), eight methylene carbon signals (δ 24.9, 26.8, 31.9, 34.6, 35.0, 41.1, 43.5, 47.4 ppm), three methine carbon signals (δ 67.8, 70.7, 71.3 ppm), ten olefinic carbon signals (δ 125.3, 117.9, 125.3, 128.6, 129.8, 130.7, 131.0, 136.0, 139.2, 143.1 ppm), and two quaternary carbon signals (δ 166.2, 211.9 ppm). Analysis of the ^{13}C NMR spectrum (Table 22) indicated the presence of one ester carbonyl carbon (δ 166.2 ppm), one ketone carbonyl carbon (δ 211.9 ppm), and ten olefinic carbons (δ 117.9-143.1 ppm). These accounted for seven of eight degrees of

unsaturation required by the molecular formula, therefore illustrating compound P035 to be monocyclic.

According to HMQC spectrum of compound P035 (Figures 148-150), the protonated carbons could be assigned as follows : H-2 (δ 5.54 ppm)-C-2 (δ 117.9 ppm), H-3 (δ 6.50 ppm)-C-3 (δ 143.1 ppm), H-4 (δ 7.28 ppm)-C-4 (δ 129.8 ppm), H-5 (δ 5.99 ppm)-C-5 (δ 139.2 ppm), 2H-6 (δ 2.46 ppm)-C-6 (δ 41.1 ppm), H-7 (δ 4.29 ppm)-C-7 (δ 71.3 ppm), H-8 (δ 5.72 ppm)-C-8 (δ 136.0 ppm), H-9 (δ 6.43 ppm)-C-9 (δ 125.3 ppm), H-10 (δ 6.09 ppm)-C-10 (δ 130.7 ppm), H-11 (δ 5.45 ppm)-C-11 (δ 127.4 ppm), 2H-12 (δ 2.39 ppm)-C-12 (δ 34.6 ppm), H-13 (δ 4.03 ppm)-C-13 (δ 67.8 ppm), 2H-14 (δ 2.53, 2.60 ppm)-C-14 (δ 47.4 ppm), 2H-16 (δ 2.42 ppm)-C-16 (δ 43.5 ppm), 2H-17 (δ 2.20 ppm)-C-17 (δ 26.8 ppm), H-18 (δ 5.34 ppm)-C-18 (δ 128.6 ppm), H-19 (δ 5.35 ppm)-C-19 (δ 131.0 ppm), 2H-20 (δ 1.90, 1.97 ppm)-C-20 (δ 31.9 ppm), 2H-21 (δ 1.38, 1.58 ppm)-C-21 (δ 24.9 ppm), 2H-22 (δ 1.48, 1.58 ppm)-C-22 (δ 35.0 ppm), H-23 (δ 4.96 ppm)-C-23 (δ 70.7 ppm), and 3H-23-Me (δ 1.17 ppm)-C-23-Me (δ 20.0 ppm).

The ^{1}H-^{1}H COSY and TOCSY spectra of compound P035 (Figures 158-160 and 168) readily allowed the assignment of the partial structures from H-2 to H-14 and from H-16 to H-23-Me (Figure 19).

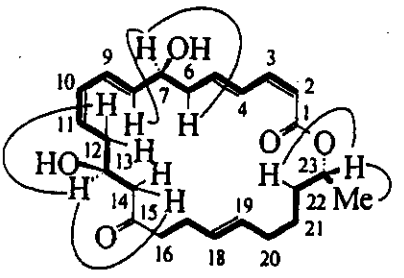

Figure 19. The important ^{1}H-^{1}H correlations (—) in the ^{1}H-^{1}H COSY spectrum and the ^{1}H-^{1}H long-range correlations (▁) in the TOCSY spectrum of macrolactin F (P035)

The HMBC spectrum ($^{n}J_{HC}$ = 8 Hz) of compound P035 (Figures 170-174) revealed the following correlations; 3H-23-Me (δ 1.17 ppm) to C-22 (δ 35.0 ppm) and C-23 (δ 70.7 ppm); H-23 (δ 4.96 ppm) to C-1 (δ 166.2 ppm) and C-21 (δ 24.9 ppm); H-2 (δ 5.54 ppm) to C-1 (δ 166.2 ppm) and C-4 (δ 129.8 ppm); H-7 (δ 4.29 ppm) to C-5 (δ 139.2 ppm), C-6 (δ 41.1 ppm), C-8 (δ 136.0 ppm), and C-9 (δ 125.3 ppm); H-13 (δ 4.03 ppm) to C-11 (δ 127.4 ppm), C-12 (δ 34.6 ppm), and C-15 (δ 211.9 ppm); and 2H-14 (δ 2.53, 2.60 ppm) and 2H-16 (δ 2.42 ppm) to C-15 (δ 211.9 ppm). The long-range correlations between protons and carbons from the HMBC spectrum are shown in Figure 20 and summarized in Table 23.

สถาบันวิทยบริการ
จุฬาลงกรณ์มหาวิทยาลัย

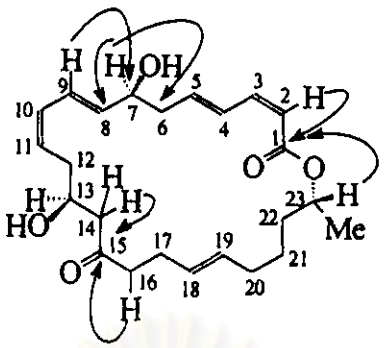

Figure 20. The important ^{1}H-^{13}C long-range correlations in the HMBC spectrum of macrolactin F (P035)

The geometries of the carbon-carbon double bonds in the α, β, γ, δ-unsaturated ester (C-1 through C-5) and the two pairs of conjugated dienes (C-8 to C-11 and C-18 to C-19) were assigned on the basis of their readily measured ^{1}H coupling constants: 10.8-11.6 Hz for *Z* and 15.3-15.4 Hz for *E*. The expansion of ^{1}H NMR spectrum of compound P035 (Figure 138) displayed the coupling pattern between olefinic protons of α, β, γ, δ-unsaturated ester and conjugated dienes as follows: H-2 (δ 5.54 ppm) to H-3 (δ 6.50 ppm) with the coupling constant of 11.6 Hz; H-4 (δ 7.23 ppm) to H-5 (δ 5.99 ppm) with the coupling constant of 15.3 Hz; H-8 (δ 5.72 ppm) to H-9 (δ 6.43 ppm) with the coupling constant of 15.3 Hz; H-10 (δ 6.09 ppm) to H-11 (δ 5.45 ppm) with the coupling constant of 10.8 Hz; and H-18 (δ 5.34 ppm) to H-19 (δ 5.35 ppm) with the coupling constant of 15.4 Hz. It could be concluded that the geometries of proton-proton on double bonds C-2=C-3 and C-10=C-11 are *Z*, while those of C-4=C-5, C-8=C-9, and C-18=C-19 are *E*.

The point of cyclization of the lactone in a compound P035 was indicated by the downfield shift of H-23 at δ 4.96 ppm, which was also clearly coupled (J = 6.4 Hz) to the 23-Me. Acetylation produced a diacetylated derivative of compound P035 in which the C-7 and C-13 proton resonances shifted downfield by approximately 1 ppm. The 300 MHz ^{1}H NMR spectrum of the diacetylated derivative (in $CDCl_3$) is shown in Figure 143. As expected, the H-23 proton signal remained essentially unchanged in this derivative. This confirmed the presence of two secondary hydroxyl groups at C-7 and C-13 ,and established that the C-23 oxygen atom was part of the lactone linkage. A direct proton-carbon heteronuclear correlation (HMQC) experiment allowed assigment of the complete ^{13}C NMR spectrum of compound P035 and the correlations observed in a long-range (two and three bonds) heteronuclear correlation (HMBC) experiment were also fully consistent with the proposed structure for compound P035 (Figure 20).

The spectral data of compound P035 were identical to those of a known compound, macrolactin F, which was previously isolated from a taxonomically unidentified deep sea bacterium (Gustafson, Roman, and Fenical, 1989). The macrolactins are the polyene macrolides containing 24-membered lactone ring.

Compound P035 showed optical rotation ($[\alpha]^{25}_{D}$ –27.94°, c = 1.31 (MeOH)) similarly to that of macrolactin F ($[\alpha]_{D}$ -30.1°, c = 1.31 (MeOH)) (Gustafson, Roman, and Fenical, 1989). It can be therefore assumed that compound P035 has the same stereochemistry as that of macrolactin F, and the complete stereochemistry is 7*S*, 13*S*, 15*R*,

23*R* (Rychnovsky *et al.*, 1992). It is finally concluded that compound P035 was a known macrolactin F.

2.8.2 7-*O*-Succinyl macrolactin F (P129)

The HRFABMS (Figure 127) established the molecular formula of compound P129 as $C_{28}H_{38}O_8$ (observed *m/z* 525.2490 $(M+Na)^+$, calculated for $C_{28}H_{38}O_8Na$, 525.2464). The UV spectrum (Figure 130) exhibited λ_{max} (log ϵ) at 235 (4.17) and 261 (4.23) nm. The IR spectrum (Figure 133) confirmed the presence of hydroxyl groups (ν_{max} 3439 cm^{-1}), carboxylic carbonyl (ν_{max} 1730 cm^{-1}), and ester carbonyl moieties (ν_{max} 1710 cm^{-1}).

The 500 MHz ^1H NMR spectrum (in $CDCl_3$) of compound P129 (Figures 136 and 139) revealed one methyl proton signal (δ 1.18 ppm), twelve methylene proton signals (δ 1.34, 1.44, 1.57, 1.91, 1.97, 2.20, 2.34, 2.40, 2.48, 2.49, 255, 2.58 ppm), and thirteen methine proton signals (δ 4.01, 4.95, 5.32, 5.35, 5.41, 5.44, 5.53, 5.62, 5.88, 6.04, 6.41, 6.45, 7.19 ppm). The 75 MHz ^{13}C NMR spectrum (in $CDCl_3$) of compound P129 (Figure 143) showed twenty eight carbon signals which could be classified by the DEPT 135 spectrum (Figure 146) as one methyl carbon signal (δ 20.0 ppm), ten methylene carbon signals (δ 24.9, 27.0, 28.9, 29.6, 31.7, 34.7, 35.0, 38.4, 43.6, 47.6 ppm), three methine carbon signals (δ 68.0, 70.9, 72.5 ppm), ten olefinic carbon signals (δ 117.9, 126.5, 127.8, 128.5, 130.0, 130.5, 130.8, 131.0, 137.7, 143.0 ppm), and four quaternary carbon signals (δ 166.2, 171.0, 174.3, 211.9 ppm). Analysis of the ^{13}C NMR spectrum (Table 22) showed two ester carbonyl carbons (δ 166.2, 171.0 ppm), one carboxylic carbonyl carbon (δ 174.3 ppm), one

ketone carbonyl carbon (δ 211.9 ppm), and ten olefinic carbons (δ 117.9-143.0 ppm) assigned to two, one, one, and five double bonds, respectively. These accounted for nine of ten degrees of unsaturation required by the molecular formula, therefore illustrating compound P129 to be monocyclic.

The ^{1}H-^{1}H COSY and TOCSY spectra of compound P129 (Figures 161-1653 and 169) allowed the assignment of partial structures from H-2 to H-14 and from H-16 to H-23. The two fragments were connected by the ketone carbonyl carbon C-15 (δ 211.9 ppm) and the ester carbonyl carbon C-11 (δ 166.2 ppm). The ^{1}H-^{13}C long-range correlations from the HMBC spectrum (Figures 175-180) assured this connectivity: 2H-14 to C-15, 2H-16 to C-15 and H-2 to C-1, H-23 to C-1. The connectivity allowed the structure of compound P129 to be a member of the macrolactins.

According to the HMQC spectrum of compound P129 (Figures 151-153), the protonated carbons could be assigned in Table 22. By comparing ^{1}H and ^{13}C spectral data of compound P129 and those of compound P035, it was found that compound P129 had the extra $C_4H_4O_3$ unit consisting of two methylene carbons C-2' (δ 28.9 ppm) and C-3' (δ 29.6 ppm) connected to 2H-2' and 2H-3' at the same proton chemical shifts (δ 2.58 ppm), one ester carbonyl carbon (δ 171.0 ppm), and one carboxylic carbonyl carbon (δ 174.3 ppm).

Analysis of the ^{1}H NMR spectral data (Table 22) showed the downfield shift of H-7 (from δ 4.34 ppm of compound P035 to δ 5.41 ppm of compound

P129) and the additional four equivalent protons (2H-2' and 2H-3') at δ 2.58 ppm. The ^{13}C NMR spectral data (Table 22) showed the additional carbon signals at δ 28.9 (C-2'), 29.6 (C-3'), 171.0 (C-1'), and 174.3 (C-4') ppm. The HMQC NMR spectrum of compound P129 revealed connectivity of the four protons (2H-2' and 2H-3') at δ 2.58 ppm to the methylene carbons at δ 28.9 (C-2') and δ 29.6 (C-3') ppm, respectively.

In a similar fashion to that of compound P035, the connectivity and the assignment of the quaternary carbons of each fragment of compound P129 could be successfully demonstrated by the HMBC spectrum ($^nJ_{HC}$ = 8 Hz) (Figures 175-180). The long-range correlations of the methylene protons at δ 2.58 ppm (2H-2' and 2H-3') to the carbonyl carbons at δ 171.0 (C-1') and 174.3 (C-4') ppm indicated the presence of the succinic acid half-ester moiety in compound P129 which was supported by the IR spectrum of compound P129 (Figure 133), exhibiting intensely broad hydroxyl absorption from 3500 to 2500 cm^{-1}, carboxylic carbonyl absorption at 1730 cm^{-1}, and ester carbonyl absorption at 1710 cm^{-1}. Assignment of the esterification of the succinic acid group at C-7 hydroxyl group was confirmed by the downfield shift of H-7 (δ 5.41 ppm) in compound P129 comparative to the chemical shift of H-7 (δ 4.34 ppm) in compound P035 and also by the long-range correlation of H-7 to the carbonyl carbon at δ 171.0 (C-1') ppm in the HMBC spectrum of compound P129 (Figure 180). Compound P129 was therefore 7-*O*-succinyl macrolactin F, a new analogue of macrolactins.

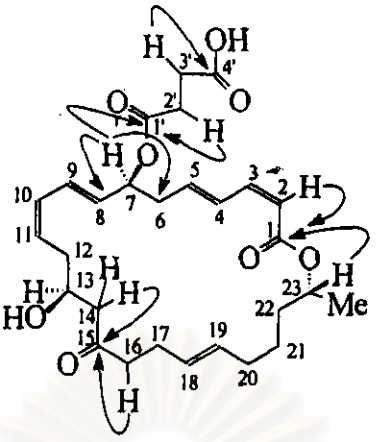

Figure 21. The important ^{1}H-^{13}C long-range correlations in the HMBC spectrum of 7-*O*-succinyl macrolactin F (P129)

The ^{1}H NMR data of compound P129 with analysis of coupling constant revealed that the geometries of the carbon-carbon double bonds in the α, β, γ, δ-unsaturated ester (C-1 through C-5) and the two pairs of conjugated dienes (C-8 to C-11) of compound P129 were similar to those of compound P035. The expansion of ^{1}H NMR spectrum of compound P129 (Figure 139) displayed the correlation between olefinic protons of α, β, γ, δ-unsaturated ester and conjugated dienes.

Compound P129 showed optical rotation ($[\alpha]^{25}_{D}$ –24.4°, c = 0.50 (MeOH)) similarly to that of compound P035 ($[\alpha]^{25}_{D}$ –27.94°, c = 1.31 (MeOH)); it can be therefore assumed that compound P129 has the same orientation as that of compound P035.

Table 22. ^{1}H and ^{13}C NMR spectral data of macrolactin F (P035), 7-*O*-succinyl macrolactin F (P129), and macrolactin F (in $CDCl_3$)

Position	Macrolactin F (P035)[a]		7-*O*-Succinyl macrolactin F (P129)[b]		Macrolactin F[c]	
	δ_C (ppm)	δ_H (ppm), mult (*J* in Hz)	δ_C (ppm)	δ_H (ppm), mult (*J* in Hz)	δ_C (ppm)	δ_H (ppm), mult (*J* in Hz)
1	166.2	-	166.2	-	166.3	-
2	117.9	5.54, d (11.6)	117.9	5.53, d (11.6)	117.8	5.59, d (11.5)
3	143.1	6.50, dd (11.3, 11.6)	143.0	6.45, dd (10.9, 11.6)	143.2	6.54, dd (11.2, 11.5)
4	129.8	7.28, dd (11.3, 15.3)	130.0	7.19, dd (10.9, 15.5)	128.7	7.29, dd (11.2, 15.1)
5	139.2	5.99, dt (7.3, 15.3)	137.7	5.88, dt (7.5, 15.5)	139.4	6.06, dt (7.6, 15.1)
6	41.1	2.46, 2H, m[d]	38.4	2.48, 2H, m	41.2	2.48, 2H, m
7	71.3	4.29, dt (5.8, 6.1)	72.5	5.41, m	71.3	4.34, dt (5.8, 6.1)
8	136.0	5.72, dd (5.8, 15.3)	130.8	5.62, dd (5.2, 15.2)	136.2	5.77, dd (6.1, 15.1)
9	125.3	6.43, dd (11.0, 15.3)	126.5	6.41, tdd (1.2, 10.9, 15.2)	125.3	6.49, dd (11.1, 15.1)
10	130.7	6.09, dd (10.8, 11.0)	130.5	6.04, dd (10.8, 10.9)	130.8	6.14, dd (10.8, 11.1)
11	127.4	5.45, dt (8.2, 10.8)	127.8	5.44, dt (8.2, 10.8)	127.3	5.51, dt (8.3, 10.8)
12	34.6	2.39, 2H, m[d]	34.7	2.34, 2H, m[d]	35.1	2.46, 2H, m
13	67.8	4.03, m	68.0	4.01, m	67.9	4.06, m
14	47.4	2.53, dd (7.5, 17.2) 2.60, dd (4.3, 17.2)	47.6	2.49, dd (7.9, 17.4) 2.55, dd (4.0, 17.4)	43.8	2.53, dd (7.6, 17.0) 2.61, dd (4.0, 17.0)
15	211.9	-	211.9	-	211.8	-
16	43.5	2.42, 2H, m[d]	43.6	2.40, 2H, t (7.3)	47.6	2.43, 2H, m
17	26.8	2.20, 2H, m[d]	27.0	2.20, 2H, m[d]	26.8	2.26, 2H, m
18	128.6	5.34, dd (5.2, 15.4)	128.5	5.32, dd (5.5, 15.3)	129.7	5.39
19	131.0	5.35, dd (5.7, 15.4)	131.0	5.35, dd (5.5, 15.3)	131.0	5.41
20	31.9	1.90, m 1.97, m	31.7	1.91, m 1.97, m	31.9	1.93, m 2.01, m
21	24.9	1.38, m[d] 1.58, m[d]	24.9	1.34, 2H, m	24.9	1.45, 2H, m
22	35.0	1.48, m[d] 1.58, m[d]	35.0	1.44, m 1.57, m	34.7	1.40, m 1.63, m
23	70.7	4.96, m	70.9	4.95, m	70.8	5.00, m
23-Me	20.0	1.17, 3H, d (6.4)	20.0	1.18, 3H, d (6.4)	20.0	1.25, 3H, d (6.1)

Table 22. (continued)

Position	Macrolactin F (P035)[a]		7-*O*-Succinyl macrolactin F (P129)[b]		Macrolactin F[c]	
	δ_C (ppm)	δ_H (ppm), mult (*J* in Hz)	δ_C (ppm)	δ_H (ppm), mult (*J* in Hz)	δ_C (ppm)	δ_H (ppm), mult (*J* in Hz)
1'	-	-	171.0	-	-	-
2'	-	-	28.9[d]	2.58, 4H, br s	-	-
3'	-	-	29.6[d]		-	-
4'	-	-	174.3	-	-	-

[a]Data were recorded at 400 MHz (^{1}H) and 75 MHz (^{13}C).
[b]Data were recorded at 500 MHz (^{1}H) and 75 MHz (^{13}C).
[c]Macrolactin F from Gustafson, Roman, and Fenical, 1989.
[d]Overlapping signals.
[e]Assignments may be interchangeable.

Table 23. The long-range corelations between protons and carbons from the HMBC spectra of macrolactin F (P035) and 7-*O*-succinyl macrolactin F (P129)

Position	Macrolactin F (P035)			7-*O*-Succinyl macrolactin F (P129)		
	δ_C (ppm)	δ_H (ppm)	Long-range correlations in HMBC spectrum[a]	δ_C (ppm)	δ_H (ppm)	Long-range correlations in HMBC spectrum[b]
1	166.2	-		166.2	-	
2	117.9	5.54	C-1, C-4	117.9	5.53	C-1, C-3, C-4
3	143.1	6.50	C-1, C-4, C-5	143.0	6.45	C-1, C-4, C-5
4	129.8	7.23	C-2, C-3, C-6	130.0	7.19	C-2, C-3, C-5
5	139.2	5.99	C-3, C-6, C-7, C-8	137.7	5.88	C-3, C-6, C-7
6	41.1	2.46	C-3, C-5, C-7, C-8	38.4	2.48	C-4, C-5, C-7, C-8
7	71.3	4.29	C-5, C-6, C-8, C-9	72.5	5.41	C-5, C-6, C-8, C-9, C-1'
8	136.0	5.72	C-6, C-7, C-10	130.8	5.62	C-6, C-7, C-9, C-10
9	125.3	6.43	C-7, C-10, C-11	126.5	6.41	C-7, C-8, C-10, C-11
10	130.7	6.09	C-8, C-9, C-12	130.5	6.04	C-8, C-9, C-12
11	127.4	5.45	C-9, C-10, C-12, C-13	127.8	5.44	C-9, C-10, C-12
12	34.6	2.39	C-10, C-11, C13, C-14	34.7	2.34	C-10, C-11, C-13
13	67.8	4.03	C-11, C-12, C-15		4.01	-

Table 23. (continued)

Position	Macrolactin F (P035)			7-*O*-Succinyl macrolactin F (P129)		
	δ_C (ppm)	δ_H (ppm)	Long-range correlations in HMBC spectrum[a]	δ_C (ppm)	δ_H (ppm)	Long-range correlations in HMBC spectrum[b]
14	47.4	2.53 2.60	C-12, C-15, C-16	68.0 47.6	2.49 2.55	C-12, C-13, C-15
15	211.9	-		211.9	-	
16	43.5	2.42	C-14, C-15, C-17, C-18	43.6	2.40	C-14, C-15, C-17, C-18
17	26.8	2.20	C-15, C-16, C-18	27.0	2.20	C-16, C-18, C-19
18	128.6	5.34	C-16, C-17, C-19, C-20	128.5	5.32	C-17, C-19, C-20
19	131.0	5.35	C-17, C-18, C-20, C-21	131.0	5.35	C-17, C-18, C-20
20	31.9	1.90 1.97	C-18, C-21, C-22	31.7	1.91 1.97	C-18, C-19
21	24.9	1.38 1.58	C-20, C-22, C-23	24.9	1.34	C-19, C-20, C-22, C-23-Me C-20, C-21, C-23-Me
22	35.0	1.48 1.58	C-20, C-21, C-23	35.0	1.44 1.57	C-20, C-21, C-23-Me
23	70.7	4.96	C-1, C-21	70.9	4.95	C-1, C-21, C-23-Me
23-Me	20.0	1.17	C-22, C-23	20.0	1.18	C-21, C-23
1'	-	-	-	171.0	-	
2'	-	-	-	28.9	2.58	C-7, C-1', C-4'
3'	-	-	-	29.6		
4'	-	-	-	174.3	-	

[a]Data were recorded at 300 MHz ($^nJ_{HC}$ = 8 Hz).
[b]Data were recorded at 500 MHz ($^nJ_{HC}$ = 8 Hz).

ศูนย์วิทยทรัพยากร
จุฬาลงกรณ์มหาวิทยาลัย

2.8.3 7-*O*-Succinyl macrolactin A (P103)

The HRFABMS (Figure 128) established the molecular formula of compound P103 as $C_{28}H_{38}O_8$ (observed *m/z* 525.2421 $(M+Na)^+$, calculated for $C_{28}H_{38}O_8Na$, 525.2464). The UV spectrum (Figure 131) exhibited λ_{max} (log ϵ) at 229 (4.57) and 261 (4.18) nm. The IR spectrum (Figure 134) exhibited the maximum absorption bands at 3295 cm^{-1} (OH streching), 1730 cm^{-1} (carboxylic carbonyl streching), 1700 and 1667 cm^{-1} (ester carbonyl streching).

As seen on the 300 MHz ^1H NMR spectrum (in $CDCl_3$) of compound P103 (Figures 137 and 140), there were one methyl proton signal (δ 1.27 ppm), eleven methylene proton signals (δ 1.45, 1.55, 1.58, 1.82, 2.08, 2.20, 2.40, 2.55, 2.65, 2.70, 2.92 ppm), and fourteen methine proton signals (δ 4.09, 4.54, 4.98, 5.36, 5.53, 5.54, 5.59, 5.68, 5.99, 6.02, 6.09, 6.48, 6.59, 7.08 ppm). The 75 MHz ^{13}C NMR spectrum (in $CDCl_3$) of compound P103 (Figure 144) showed twenty eight carbon signals which could be classified by DEPT 135 spectrum (Figure 147) as one methyl carbon signal (δ 20.0 ppm), eight methylene carbon signals (δ 24.5, 28.8, 29.7, 32.0, 34.5, 34.9, 39.1, 39.4 ppm), four methine carbon signals (δ 70.2, 70.6, 71.5, 72.3 ppm), twelve olefinic carbon signals (δ 118.5, 124.9, 127.3, 129.8, 130.0, 130.1, 130.8, 131.3, 131.9, 135.2, 137.7, 141.8 ppm), and three quaternary carbon signals (δ 166.3, 170.8, 174.8 ppm). Analysis of the ^{13}C NMR spectrum (Table 24) showed two ester carbonyl carbons (δ 166.3, 170.8 ppm), one carboxylic carbonyl carbon (δ 174.8 ppm), and twelve olefinic carbons (δ 118.5-141.8 ppm) assigned to two, one, and six double bonds, respectively. These accounted for nine of ten degrees of unsaturation required by the molecular formula, therefore implying compound P103 to be monocyclic.

Analysis of the ^{1}H, ^{13}C, and HMQC spectral data of compound P103 (Table 24) suggested that this compound was similar to those of compound P129, except that the ketone carbonyl carbon C-15 (δ 211.9 ppm), and the methylene carbons C-16 (δ 43.6 ppm) and C-17 (δ 27.0 ppm) of compound P129 were replaced by the oxymethine carbon C-15 (δ 7.02 ppm), the olefinic carbons C-16 (δ 131.9 ppm) and C-17 (δ 131.3 ppm), respectively.

The ^{1}H-^{1}H COSY spectrum of compound P103 (Figures 164-167) exhibited the connectivity from H-2 through H-23; H-23 to H-23-Me; 2H-2' to 2H-3'as shown in Figure 22.

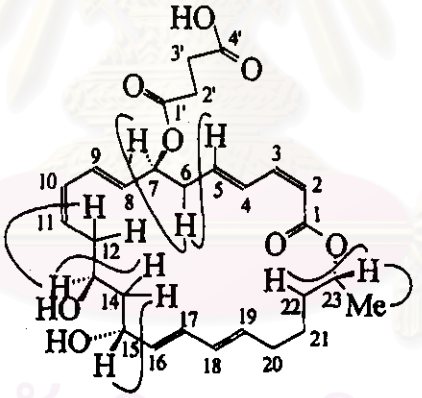

Figure 22. The important ^{1}H-^{1}H correlations (—) in the ^{1}H-^{1}H COSY spectrum of 7-*O*-succinyl macrolactin A (P103)

The connectivity and the assignment of the quaternary carbons of each fragment of compound P103 were readily demonstrated by the HMBC spectrum ($^{n}J_{HC}$ = 8 Hz) (Figures 183-187) as shown in Table 24. The long-range correlations of the methine protons at δ 5.53 (H-16) and 6.09 (H-17) ppm to the methine carbons at δ 70.2 (C-15), 130.0 (C-18), 135.2 (C-19) ppm suggested the connectivity of C-15 through C-19.

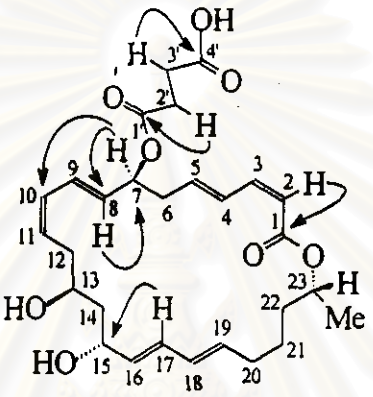

Figure 23. The important ^{1}H-^{13}C long-range correlations in the HMBC spectrum of 7-*O*-succinyl macrolactin A (P103)

The ^{1}H and ^{13}C NMR spectra of compound P103 were similar to those of macrolactin A (Gustafson, Roman, and Fenical, 1989). However additional methylene protons (δ 2.65, 2.70 ppm) and four carbons (δ 28.8, 29.7, 170.8, 174.8 ppm) were observed prominently on the ^{1}H and ^{13}C NMR spectral data of compound P103, respectively. The appearance of the succinic acid half-ester fragment in compound P103 was defined by 2D NMR studies, employing the ^{1}H-^{1}H COSY, HMQC, and HMBC techniques. The ^{1}H NMR signals at δ 2.65 (2H-2') and 2.75 (2H-3') ppm, and the ^{13}C NMR signals at δ 28.8 (C-2'), 29.7 (C-3'), 170.8 (C-1') and 174.8 (C-4') ppm were of the succinyl group. The long-range

correlations of the methylene protons at δ 2.65 (2H-2') and 2.70 (2H-3') ppm to the carbonyl carbons at δ 170.8 (C-1') and 174.8 (C-4') ppm confirmed the partial structure of C-1' through C-4'. The attachment of the succinyl group at the C-7 hydroxyl group was also secured by the downfield shift of H-7 at δ 5.54 ppm. Further 2D NMR analyses suggested that the macrolide ring of compound P103 was identical to that of macrolactin A isolated from a taxonomically unidentified deep sea bacterium (Gustafson, Roman, and Fenical, 1989). The absence of the ketone carbonyl carbon at δ 211.9 (C-15) ppm and the presence of the oxymethine carbon at δ 70.2 (C-15) ppm, the olefinic carbons at δ 131.9 (C-16) and 131.3 (C-17) ppm, the oxymethine proton at δ 5.53 (H-15) ppm, and the olefinic protons at δ 6.09 (H-16) and 5.99 (H-17) ppm revealed the characteristic of the allylic alcohol functionality at C-15 as that in macrolactin A. Compound P103 was then assigned as a new 7-*O*-succinyl macrolactin A.

The geometries of the carbon-carbon double bonds in the α, β, γ, δ-unsaturated ester (C-1 through C-5) and the two pairs of conjugated dienes (C-8 to C-11 and C-16 to C-19) were assigned on the basis of their readily measured ^{1}H coupling constants: 10.7-11.4 Hz for *Z* and 15.0-15.1 Hz for *E*. The expansion of ^{1}H NMR spectrum of compound P103 (Figure 140) displayed the coupling pattern between olefinic protons of α, β, γ, δ-unsaturated ester and conjugated dienes as follows: H-2 (δ 5.54 ppm) to H-3 (δ 6.48 ppm) with the coupling constant of 11.4 Hz; H-4 (δ 7.08 ppm) to H-5 (δ 5.59 ppm) with the coupling constant of 15.1 Hz; H-8 (δ 5.68 ppm) to H-9 (δ 6.59 ppm) with the coupling constant of 15.0 Hz; H-10 (δ 6.02 ppm) to H-11 (δ 5.36 ppm) with the coupling constant of 10.7 Hz; and H-16 (δ 5.53 ppm) to H-17 (δ 6.09 ppm) with the coupling constant of 14.8 Hz.

It is concluded that the geometries of proton-proton on double bonds C-2=C-3 and C-10=C-11 are *Z*, while that of C-4=C-5, C-8=C-9, and C-16=C-17 are *E*.

Compound P103 showed optical rotation ($[\alpha]^{25}_{D}$ –9.6°, c = 0.18 (MeOH)) similarly to that of macrolactin A ($[\alpha]_{D}$ –9.6°, c = 1.86 (MeOH)) (Gustafson, Roman, and Fenical, 1989 and Rychnovsky *et al.*, 1992). It can be therefore assumed that compound P103 has the same stereochemistry as macrolactin A, so the absolute stereochemistry of compound P103 was 7*S*, 13*S*, 15*R*, 23*R*.

Table 24. ^{1}H and ^{13}C NMR spectral data of 7-*O*-succinyl macrolactin A (P103) and macrolactin A (in $CDCl_3$), and the ^{1}H-^{13}C long-range correlations from the HMBC spectrum ($^{n}J_{HC}$ = 8 Hz) of 7-*O*-succinyl macrolactin A (P103)

Position	7-O-Succinyl macrolactin A (P103)[a]			Macrolactin A[b]	
	δ_C (ppm)	δ_H (ppm), mult (*J* in Hz)	Long-range correlations in HMBC spectrum	δ_C (ppm)	δ_H (ppm), mult (*J* in Hz)
1	166.3	-		116.3	-
2	118.5	5.54, d (11.4)	C-1	117.8	5.68, d (11.2)
3	141.8	6.48, dd (11.4, 11.6)	C-1, C-5	143.7	6.29, dd (11.2, 11.5)
4	129.8	7.08, dd (11.6, 15.1)	ND	129.4	7.48, dd (11.5, 14.9)
5	137.7	5.59, dt (7.1, 15.1)	C-3, C-7	142.4	5.85, dd (7.2, 7.2, 14.9)

Table 24. (continued)

Posi-tion	7-O-Succinyl macrolactin A (P103)[a]			Macrolactin A[b]	
	δ_C (ppm)	δ_H (ppm), mult (*J* in Hz)	Long-range correlations in HMBC spectrum	δ_C (ppm)	δ_H (ppm), mult (*J* in Hz)
6	39.4	2.55, 2H, dd (7.0, 7.1)	C-4, C-5	42.8	2.30, m 2.35, m
7	72.3	5.54, m[c]	C-8, C-10	71.2	4.15, m
8	130.8	5.68, dd (3.4, 15.0)	C-7, C-10	138.3	5.58, dd (4.7, 15.0)
9	124.9	6.59, dd (11.6, 15.0)	ND	124.9	6.73, dd (11.5, 15.0)
10	130.1	6.02[c]	C-8	130.6	6.04, dd (11.2, 11.5)
11	127.3	5.36, dt (5.5, 10.7)	ND	128.6	5.42, m
12	34.5	2.40, m 2.92, dt (10.7, 13.0)	ND	36.7	2.43, m 2.70, m
13	70.6	4.09, m	ND	68.8	4.03, m
14	39.1	1.58, m[c] 1.82, ddd (2.9, 9.5, 14.4)	ND	43.9	1.74, m 1.83, m
15	70.2	4.54, br t (7.1)	ND	69.2	4.62, m
16	131.9	5.53, dd (7.5, 14.8)	C-17, C-18	136.6	5.70
17	131.3	6.09[c]	C-15, C-19	131.2	6.35, dd (10.6, 15.3)
18	130.0	5.99[c]	C-19	129.6	6.08, dd (10.6, 14.8)

Table 24. (continued)

Position	7-O-Succinyl macrolactin A (P103)[a]			Macrolactin A[b]	
	δ_C (ppm)	δ_H (ppm), mult (*J* in Hz)	Long-range correlations in HMBC spectrum	δ_C (ppm)	δ_H (ppm), mult (*J* in Hz)
19	135.2	5.59[c]	C-18	133.7	5.70
20	32.0	2.08, m 2.20, m	ND	32.3	1.91, m 2.06, m
21	24.5	1.45, 2H, m[c]	ND	25.0	1.32, 2H, m[c]
22	34.9	1.55, 2H, m[c]	ND	35.3	1.32, m[c] 1.49, m
23	71.5	4.98, m	ND	70.8	5.10, m
23-Me	20.0	1.27, 3H, d (6.2)	C-21, C-22, C-23	19.9	1.09, 3H, d (6.5)
1'	170.8	-		-	-
2'	28.8[d]	2.65, 2H, m[d]	C-3'	-	-
3'	29.7[d]	2.70, 2H, m[d]	ND	-	-
4'	174.8	-		-	-

[a]Data were recorded at 300 MHz (^{1}H) and 75 MHz (^{13}C).
[b]Macrolactin A from Gustafson, Roman, and Fenical, 1989.
[c]Overlapping signal.
[d]Assignments may be interchangeable.
ND = No data.

2.9 *Cyclo*-(4-hydroxy-prolyl-4-hydroxy-prolyl-leucyl-phenylalanyl) (P132)

The HRFABMS (Figure 186) established the molecular formula of compound P132 as $C_{25}H_{34}N_4O_6$ by showing the protonated molecular ion peak at *m/z* 487.2581 $(M+H)^+$ (calculated for $C_{25}H_{35}N_4O_6$, 487.2557). The UV spectrum (Figure 187) exhibited λ_{max} (log ϵ) at 264 (2.80) and 206 (4.20) nm. The IR spectrum (Figure 188) showed the maximum absorption bands at 3365 cm^{-1} (OH streching), 3250 cm^{-1} (amide NH streching), 2958 cm^{-1} (cycloalkane streching), 1667 cm^{-1} (amide carbonyl streching), and 1455 cm^{-1}(aromatic ring streching).

The 500 MHz ^1H NMR spectrum (in $CDCl_3$) of compound P132 (Figures 189-192) exhibited two methyl proton signals (δ 0.93, 0.96 ppm), eleven methylene proton signals (δ 1.61, 2.16, 2.25, 2.41, 2.48, 3.02, 3.12, 3.18, 3.31, 3.86, 3.94 ppm), seven methine proton signals (δ 1.74, 2.91, 3.92, 4.13, 4.22, 4.29, 4.43 ppm), four aromatic methine proton signals (δ 7.16, 7.17, 7.25, 7.27 ppm), and one amide proton signal (δ 6.93 and 7.45 ppm on the 500 and 300 MHz ^1H NMR spectra, respectively) (Figures 189 and 190). The 75 MHz ^{13}C NMR spectrum (in $CDCl_3$) of compound P132 (Figure 193) showed twenty three carbon signals, and the DEPT 135 spectrum (Figure 194) revealed two methyl carbon signals (δ 21.6, 23.1 ppm), six methylene carbon signals (δ 36.8, 37.2, 40.2, 42.1, 53.7, 54.0 ppm), seven methine carbon signals (δ 24.7, 55.7, 56.1, 56.2, 58.7, 67.8, 68.1 ppm), three aromatic methine carbon signals (δ 127.3, 128.5, 129.8 ppm), and five quaternary carbon signals (δ 135.1,165.6, 167.4, 169.2, 169.4 ppm).

According to HMQC spectrum of compound P132 (Figures 195 and 196), the protonated carbons could be assigned as follows: H-2 (δ 2.91 ppm)-C-2 (δ 55.7 ppm), H-4 (δ 4.13 ppm)-C-4 (δ 56.2 ppm), H-6 (δ 3.92 ppm)-C-6 (δ 56.1 ppm), H-8 (δ 4.22 ppm)-C-8 (δ 58.7 ppm), 2H-9 (δ 2.16, 2.25 ppm)-C-9 (δ 37.2 ppm), H-10 (δ 4.29 ppm)-C-10 (δ 67.8 ppm), 2H-11 (δ 3.18, 3.86 ppm)-C-11 (δ 53.7 ppm), 2H-12 (δ 2.41, 2.48 ppm)-C-12 (δ 36.8 ppm), H-13 (δ 4.43 ppm)-C-13 (δ 68.1 ppm), 2H-14 (δ 3.31, 3.94 ppm)-C-14 (δ 54.0 ppm), 2H-15 (δ 1.61 ppm)-C-15 (δ 42.1 ppm), H-16 (δ 1.74 ppm)-C-16 (δ 24.7 ppm), 3H-17-Me (δ 0.93 ppm)-C-17-Me (δ 21.6 ppm), 3H-17'-Me (δ 0.96 ppm)-C-17'-Me (δ 23.1 ppm), 2H-18 (δ 3.02, 3.12 ppm)-C-18 (δ 40.2 ppm), H-20 and H-20' (δ 7.27 ppm)-C-20 and C-20' (δ 128.5 ppm), H-21 (δ 7.16 ppm)-C-21 (δ 129.8 ppm), H-21' (δ 7.17 ppm)-C-21' (δ 129.8 ppm), and H-22 (δ 7.25 ppm)-C-22 (δ 127.3 ppm).

The compound P132 was optically active, $[\alpha]^{25}_{D}$ +25.9° (c = 0.81 (MeOH)), and showed intense carbonyl (C=O) and amide (NH) absorptions at 1667 and 3365 cm^{-1}, respectively, typical of peptide type natural products. The molecular formula of compound P132 was $C_{25}H_{35}N_4O_6$ as analyzed by HRFABMS (observed $(M+H)^+$ at 487.2581) (Figure 186), thus having eleven degrees of unsaturation. The 300 MHz ^1H NMR spectrum (Figure 190) showed one doublet amide proton signal (δ 7.45 ppm) and the 75 MHz ^{13}C NMR spectrum (Figure 193) in combination with DEPT 135 spectrum (Figure 194) confirmed the presence of four amide carbonyl carbons (δ 165.6, 167.4, 169.2, 169.4 ppm) in compound P132. Based upon these spectral data, compound P132 was a peptide containing four amino acids. Since compound P132 gave a negative response to ninhydrin, it was likely to be a cyclic tetrapeptide.

Compound P132 possessed UV absorption (Figure 187) at 264 nm (log ϵ = 2.80) typical for a phenyl chromophore, IR absorption (Figure 188) at 1455 cm^{-1} due to aromatic ring streching, and a fragment ion at *m/z* 91 by EIMS correspond to tropylium ion. The ^{1}H and ^{13}C NMR spectra (Figures 189-193) showed four aromatic methine proton signals (δ 7.16, 7.17, 7.25, 7.27 ppm) and three aromatic methine carbon signals (δ 127.3, 128.5, 129.8 ppm), respectively. From these spectral data, compound P132 appeared to be a phenylalanine-containing cyclic tetrapeptide.

The HRFABMS of compound P132 (Figure 186) showed the fragment ion at *m/z* 453 resulted from the loss of two hydroxyl groups from the $(M+H)^{+}$ ion (*m/z* 487). The HMQC spectrum (Figures 195 and 196) showed two oxymethine signals of H-10 (δ 4.29 ppm)-C-10 (δ 67.8 ppm) and H-13 (δ 4.43 ppm)-C-13 (δ 68.1 ppm). From these data, it should be suggested that both of hydroxyl groups were attached to compound P132.

The ^{1}H-^{1}H COSY and TOCSY spectra of compound P132 (Figures 197-200) exhibited the correlations in each amino acid, showing the following connectivities: H-2 (δ 2.91 ppm)-2H-9 (δ 2.16, 2.25 ppm)-H-10 (δ 4.29 ppm)-2H-11 (δ 3.18, 3.86 ppm) in the first amino acid; H-4 (δ 4.13 ppm)-2H-12 (δ 2.41, 2.48 ppm)-H-13 (δ 4.43 ppm)-2H-14 (δ 3.31, 3.94 ppm) in the second amino acid; H-6 (δ 3.92 ppm)-2H-15 (δ 1.61 ppm)-H-16 (δ 1.74 ppm)-3H-17-Me (δ 0.93 ppm) and 3H-17'-Me (δ 0.96 ppm) in the third amino acid; H-6 (δ 3.92 ppm)-NH-c (δ 7.45 ppm); and H-8 (δ 4.22 ppm)-2H-18 (δ 3.02, 3.12 ppm)-aromatic-H-20, 20', 21, 21', 22 (δ 7.16, 7.17, 7.25, 7.27 ppm) in the last amino acid.

The complete carbon assignments of compound P132 were achieved by the analysis of the HMBC ($^{n}J_{HC}$ = 3 and 8 Hz on 300 MHz, and 4 Hz on 500 MHz) spectra (Figures 201-204). The HMBC correlations summarized in Table 25 provided assignments of the several carbons of compound P132, and were critical the establishment of amino acids sequence in compound P132. The long-range correlations obtained from the HMBC spectra of compound P132 are as follows: the first amino acid showed long-range correlations from the methine proton at δ 2.91 (H-2) ppm to the amide carbonyl carbon at δ 169.2 (C-1) ppm and the methylene carbon at δ 37.2 (C-9) ppm; and the long-range correlations from the methine proton at δ 4.29 (H-10) ppm to the both methylene carbons at δ 37.2 (C-9) and 53.7 (C-11) ppm: the second amino acid showed long-range correlations from the methine proton at δ 4.13 (H-4) ppm to the amide carbonyl carbon at δ 169.4 (C-3) ppm and the methylene carbon at δ 36.8 (C-12) ppm; and the long-range correlations from methine proton at δ 4.43 (H-13) ppm to the both methylene carbons at δ 36.8 (C-12) and 54.0 (C-14) ppm: the third amino acid showed long-range correlations from methine proton at δ 3.92 (H-6) ppm to the amide carbonyl carbon at δ 167.4 (C-5) ppm and the methylene carbon at δ 42.1 (C-15) ppm; the long-range correlations from the methine proton at δ 1.74 (H-16) ppm to the methylene carbon at δ 42.1 (C-15) ppm and the both methyl carbons at δ 21.6 (C-17-Me) and 23.1 (C-17'-Me) ppm; and the long-range correlation of the amide proton at δ 7.45 (NH-c) ppm to the methine carbon at δ 56.1 (C-6) ppm: the last amino acid showed long-range correlation from the methine proton at δ 4.22 (H-8) ppm to the amide carbonyl carbon at δ 165.6 (C-7) ppm; and the long-range correlations from the methylene protons δ 3.02, 3.12 (2H-18) ppm to the amide carbonyl carbon at δ 165.6 (C-7), the methine carbon at δ 58.7 (C-8) ppm, and the

quaternary carbon at δ 135.1 (C-19). Based on the ^{1}H, ^{13}C, ^{1}H-^{1}H COSY, TOCSY, and HMBC spectral data of compound P132, it was concluded that compound P132 was a cyclic tetrapeptide containing sequentially amino acids, hydroxyproline, hydroxyproline, leucine, and phenylalanine. The amino acids sequence in compound P132 was readily established by the HMBC spectrum. The long-range correlations were observed from two methylene protons at δ 3.31 (H-14a) and 3.94 (H-14b) ppm to the amide carbonyl carbon at δ 167.4 (C-5) ppm; from the methine proton at δ 4.22 (H-8) ppm to the amide carbonyl carbon at δ 169.2 (C-1) ppm; and from the amide proton at δ 7.45 (NH-c) ppm to the amide carbonyl carbon at δ 165.6 (C-7) ppm.

The HMBC spectra of compound P132 (Figures 201-204) allowed the following assignments: the long-range correlations from 2H-14 (δ 3.31, 3.94 ppm) to C-5 (δ 167.4 ppm) established the vicinity of the second hydroxyproline and leucine, while the long-range correlation from H-6 (δ 3.92 ppm) to C-5 (δ 167.4 ppm) established H-6 and C-5 as α-proton and amide carbonyl carbon of leucine, respectively: the correlations from NH-c (δ 7.45 ppm) to C-6 (δ 56.1 ppm) and C-7 (δ 165.6 ppm) established the vicinity of leucine and phenylalanine, while the long-range correlations from H-8 (δ 4.22 ppm) to C-7 (δ 165.7 ppm) established H-8 and C-7 as α-proton and amide carbonyl carbon of phenylalanine, respectively: and the long-range correlations from H-8 (4.22 ppm) to C-1 (δ 169.2 ppm) established the vicity of phenylalanine and the first hydroxyproline, while the long-range correlations from H-2 (δ 2.91 ppm) to C-1 (δ 169.2 ppm) establised H-2 and C-1 as α-proton and carbonyl carbon of the first hydroxyproline, respectively. The remaining amide carbonyl carbon (δ 169.4 ppm), to which no direct long-range correlations between the first

hydroxyproline and the second hydroxyproline, were observed must be assigned to the C-3 position of compound P132. The HMBC correlations of compound P132 are shown in Figure 24. These spectral data revealed chemical structure of compound P132 to be *cyclo*-(4-hydroxy-prolyl-4-hydroxy-prolyl-leucyl-phenylalanyl) (Figure 24).

The relative configuration of three methine protons in compound P132 (H-2, H-6, and H-8) at δ 2.91, 3.92, and 4.22 ppm, respectively, was proposed by the anisotropy effect between H-2 and the aromatic ring of the phenylalanine. The proton chemical shift of H-2 was upfield to δ 2.91 ppm, while that of H-6 was downfield to 3.92 ppm. The upfield shift of H-2 suggested that H-2 may be in the same plane of the aromatic ring of the phenylalanine, therefore causing an anisotropy effect, whereas the downfield signals of H-6 suggested that H-6 may be in the different plane of that aromatic ring (Figure 25). The configuration of H-4 in Figure 25 was assumed to be in the same plane of H-6 and H-8 since this minimized energy conformation allows the aromatic ring to shield H-2.

Cyclic tetrapeptides are a chemical class well recognized from bacteria and fungi, and also appear to represent a common chemical theme in the cyanobacteria (blue-green algae) (Gerwick *et al*, 1992). The compound P132 is proposed to be a new cyclic tetrapeptide composed of two hydroxyprolines, leucine and phenylalanine isolated from marine *Bacillus* sp. Compound P132 was named as *cyclo*-(4-hydroxy-prolyl-4-hydroxy-prolyl-leucyl-phenylalanyl).

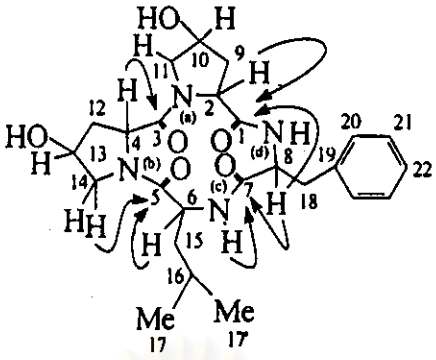

Figure 24. The important ^{1}H-^{13}C long-range correlations in the HMBC spectra of *cyclo*-(4-hydroxy-prolyl-4-hydroxy-prolyl-leucyl-phenylalanyl) (P132)

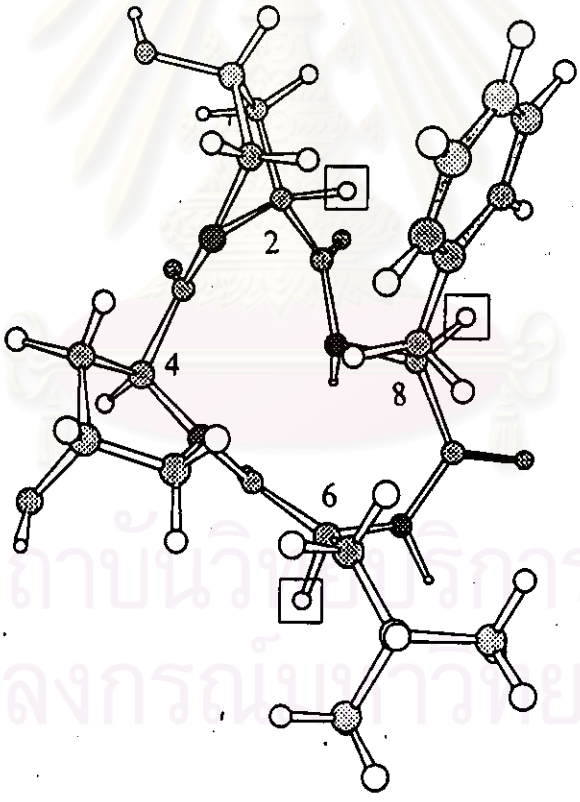

Figure 25. The relative stereochemistry of *cyclo*-(4-hydroxy-prolyl-4-hydroxy-prolyl-leucyl-phenylalanyl) (P132) in three-dimensional structure

Table 25. ^{1}H, ^{13}C NMR spectral data (in $CDCl_3$), and the long-range correlations between protons and carbons of *cyclo*-(4-hydroxy-prolyl-4-hydroxy-prolyl-leucyl-phenylalanyl) (P132)

Position	δ_C (ppm)[a]	δ_H (ppm), mult. (J in Hz)[b]	Long-range correlations in HMBC spectra[c]
1	169.2	-	
2	55.7	2.91, dd (7.1, 9.0)	C-1, C-9
3	169.4	-	
4	56.2	4.13, dd (5.0, 9.4)	C-3, C-12
5	167.4	-	
6	56.1	3.92, ddd (4.4, 6.9, 8.7)	C-5, C-15, C-16
7	165.6	-	
8	58.7	4.22, dt (4.2, 6.1)	C-1, C-7, C-18
9a	37.2	2.16, dddd (1.5, 2.7, 7.1, 14.1)	C-2, C-10, C-11
9b		2.25, ddd (5.2, 9.0, 14.1)	C-1
10	67.8	4.29, tt (2.7, 5.2)	C-9, C-11
11a	53.7	3.18, dd (5.2, 12.8)	C-9, C-14
11b		3.86, ddd (1.5, 2.7, 12.8)	C-3
12a	36.8	2.41, ddd (5.0, 9.4, 13.9)	C-4, C-14
12b		2.48, dddd (2.0, 3.0, 5.0, 13.9)	C-3
13	68.1	4.43, tt (3.0, 5.0)	C-12, C-14
14a	54.8	3.31, dd (5.0, 12.4)	C-5, C-12
14b		3.94, ddd (2.0, 3.0, 12.4)[d]	

Table 25. (continued)

Position	δ_C (ppm)[a]	δ_H (ppm), mult. (J in Hz)[b]	Long-range correlations in HMBC spectra[c]
15	42.1	1.61, 2H, m	C-6, C-16, C-17-Me, C-17'-Me, C-5
16	24.7	1.74, m	C-6, C-15, C-17-Me, C-17'-Me
17-Me	21.6	0.93, 3H, d (6.7)	C-15, C-16, C-17'-Me
17'-Me	23.1	0.96, 3H, d (6.4)	C-15, C-16, C-17-Me
18a	40.2	3.02, dd (4.2, 13.7)	C-7, C-8, C-19
18b		3.12, dd (6.1, 13.7)	C-7
19	135.1	-	
20, 20'	128.5	7.27, 2H, m[d]	C-18, C-19, C-21, C-21', C-22
21	129.8[d]	7.16, d (7.0)	C-8, C-18, C-19, C-20, C-20', C-22
21'	129.8[d]	7.17, d (7.9)	
22	127.3	7.25, m[d]	C-18, C-19, C-20, C-20', C-21, C-21'
NH-c	-	6.93, br s[a] or 7.45, d (4.4)[e]	C-6, C-7
NH-d	-	7.24, br s	C-1

[a]Data were recorded at 500 MHz (^{1}H).
[b]Data were recorded at 75 MHz (^{13}C).
[c]Data were recorded at 300 MHz ($^nJ_{HC}$ = 3 and 8 Hz) and 500 MHz ($^nJ_{HC}$ = 4 Hz).
[d]Overlapping signal.
[e]Data were recorded at 300 MHz (^{1}H).

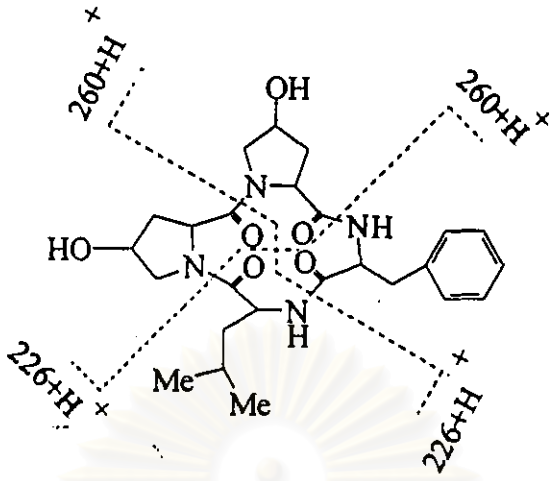

Figure 26. Proposed mass fragmentation of *cyclo*-(4-hydroxy-prolyl-4-hydroxy-prolyl-leucyl-phenylalanyl) (P132)

สถาบันวิทยบริการ
จุฬาลงกรณ์มหาวิทยาลัย

3. Biological activity

The results of biological activities including anti-herpes simplex virus type I (anti-HSV I) and type II (anti-HSV II), antimicrobial, antimalarial, and cytotoxic activities of crude extracts, and pure compounds (DKPs) obtained from marine bacteria (Sc004, Sc018 and Sc026) and a synthetic diketopiperazine (DKP) are shown in Tables 26-29.

From the screening tests of anti-HSV activity, the CH_2Cl_2 extract and the MeOH extract obtained from the strain Sc018, the EtOAc extract and the BuOH extract obtained from the strain Sc004, exhibited anti-HSV activity. The results are presented in Table 26. Based on bioassay-directed fractionation, three active compounds (F017, F018, and F019) were purified from an active fraction, F010, which was fractionated from the active CH_2Cl_2 extract of the strain Sc018. A pure compound, S147, and a fraction, S142, were isolated from the active BuOH extract of the strain Sc004. Eight pure compounds isolated from the EtOAc extract of the strain Sc026, including macrolactin F (P035), 7-*O*-succinyl macrolactin F (P129), 7-*O*-succinyl macrolactin A (P103), *cyclo*-(L-prolyl-D-leucyl) (P049), *cyclo*-(L-prolyl-glycyl) (P056WC), *cyclo*-(D-prolyl-L-phenylalanyl) (P348), *cyclo*-(L-prolyl-L-tryptophanyl) (P350), and *cyclo*-(D-prolyl-L-tryptophanyl) (P352) showed anti-HSV activity.

สถาบันวิทยบริการ
จุฬาลงกรณ์มหาวิทยาลัย

Table 26. Anti-herpes simplex virus (anti-HSV) activity and cytotoxic activity of crude extracts and chemical compounds obtained from marine bacteria (Sc004, Sc018 and Sc026), and a synthetic diketopiperazine (dkp27)

Fractions or compounds	Cytotoxic activity against Vero cells (μg/ml)	Anti-HSV I activity	Anti-HSV II activity
CH_2Cl_2 extract (Sc018)[a]	>20	++	++
MeOH extract (Sc018)[a]	>20	++	++
F010[a]	>20	++	++
F017[b, c]	>50	+++	+
F018[b, c]	>50	+++	+
F019[b, c]	>50	+++	+
EtOAc extract (Sc004)[a]	>50	+	-
BuOH extract (Sc004)[a]	>50	+	+
S142[b]	>50	++	+
S147[b, c]	>50	+	+
EtOAc extract (Sc026)[a]	>50	-	-
BuOH extract (Sc026)[a]	>50	-	+
P035[b, c]	>50	+++	+++
P049[b, c]	>50	++	++
P056 WC[b, c]	>50	++	++
P103[b, c]	>50	+++	++
P129[b, c]	>50	-	+
P348[b, c]	>50	++	++
P350[b, c]	>50	+++	+

Table 26. (continued)

Fractions or compounds	Cytotoxic activity against Vero cells (μg/ml)	Anti-HSV I activity	Anti-HSV II activity
P352 [b, c]	>50	+	+
dkp27 [b, c]	>50	+++	+

Acyclovir was used as a positive control (100% inhibition).

[a]Data from sulforhodamine B (SRB) colorimetric method.
- = inactive
+ = inhibition >20%
++ = inhibition >35%
+++ = active inhibition >50%

[b]Data from plaque reduction method.
- = inactive
+ = 25% inhibition
++ = 50% inhibition
+++ = 75% inhibition

[c]Pure compound.

From the antimicrobial activity screening tests, the EtOAc extract and the BuOH extract, obtained from the fermentation broth of the marine *Bacillus* sp. Sc026, exhibited antibacterial activity against *Staphylococcus aureus* ATCC 25923 and *Bacillus subtilis* ATCC 6633, but both extracts were inactive against *Escherichia coli* ATCC 25922 and *Candida albicans* ATCC 10231. The results are shown in Table 27. According to these results, the isolation of bioactive compounds from these crude extracts was guided by using the antibacterial activity against *S. aureus* and *B. subtilis*. Agar diffusion method and autobiographic method were used for examining the inhibition zones of active fractions and active spots, respectively (Tables 27 and 28). Guided by these methods, active compounds P035, P103, and P129 were purified from the active EtOAc extract.

Table 27. Antimicrobial activity of crude extracts and chemical compounds obtained from marine *Bacillus* sp. Sc026 using an agar diffusion method

Fractions or compounds	Concentrations (μg/disk)	Inhibition zones (mm)			
		S. aureus ATCC 25923	*B. subtilis* ATCC 6633	*E. coli* ATCC 25922	*C. albicans* ATCC 10231
EtOAc extract (Sc 026)	1,000	25.0	9.5	-	-
BuOH extract (Sc 026)	1,000	14.0	-	-	-
P003	1,000	-	ND	ND	ND
P004	1,000	-	ND	ND	ND
P005	1,000	-	ND	ND	ND
P006	1,000	10.0	ND	ND	ND
P007	1,000	22.5	ND	ND	ND
P008	1,000	20.0	ND	ND	ND
P009	1,000	19.5	ND	ND	ND
P035[a]	100	28.0	8.0	ND	ND
P103[a]	50	24.0	10.1	ND	ND
P106	100	-	26.5	ND	ND
P129[a]	100	8.0	8.5	ND	ND
P132[a]	100	-	-	ND	ND

[a]Pure compound.
- = Inactive.
ND = Not determined.

Table 28. Antimicrobial activity of fractions obtained from marine *Bacillus* sp. Sc026 using autobiographic method (1 mg/TLC plate)

Fractions	Test microorganisms		R_f values of clear zone	Solvent systems
	S. aureus ATCC 25923	*B. subtilis* ATCC 6633		
P003	-	-	-	-
P004	-	-	-	-
P005	-	+	0.60-0.80	A
P006	+	ND	0.30-0.50	B
P007	+	ND	0.20-0.80	B
P009	+	ND	0.00-0.90	C
P015	-	ND	-	-
P016	+	ND	0.20-0.80	D
P017	+	ND	0.20-0.50	D
P018	+	ND	0.40-0.50	D
P019	-	ND	-	-
P020	-	ND	-	-
P021	+	ND	0.10-06.60	B
P022	+	ND	0.20-0.70	B
P023	+	ND	0.20-0.70	B
P024	-	ND	-	-
P025	-	ND	-	-
P026	+	ND	0.20-0.80	B
P027	+	ND	0.30-0.90	B
P028	+	ND	0.10-0.80	B

สถาบันวิทยบริการ
จุฬาลงกรณ์มหาวิทยาลัย

Table 28. (continued)

Fractions	Test microorganisms		R_f values of clear zone	Solvent systems
	S. aureus	*B. subtilis*		
P029	+	ND	0.40-0.50	B
P030	+	ND	0.10-0.50	B
P031	+	ND	0.10-0.80	B
P226	+	ND	0.20-0.50	E
P267	+	ND	0.10-0.50	E
P268	+	ND	0.30-0.60	E
P269	+	ND	0.20-0.50	E
P270	+	ND	0.20-0.60	E
P271	-	ND	-	-

A = $CHCl_3$:Hexane:MeOH (9:1:2)
B = $CHCl_3$:EtOAc (1:4)
C = EtOAc:MeOH (1:1)
D = CH_2Cl_2:MeOH (9:1)
E = $CHCl_3$:MeOH (7:3)
- = Absence of inhibition zone.
+ = Presence of inhibition zone.
ND = Not determined.

It was previously reported that several macrolactins exhibited cytotoxic activity towards B16-F10 murine melanoma cell lines (Gustafson, Roman, and Fenical, 1989). As part of our continuing interest in exploring antimalarial screening, a known macrolactin F (P035), and 2'-deoxyadenosine (S147) showed an inhibitory effect against *in vitro* growth of *Plasmodium falciparum* K1 multidrug resistant strain with ED_{50} at 11.4 and 4.8 μg/ml, respectively (Table 29). The antimalarial activity of 2'-deoxyadenosine was at least 2-fold more active than of macrolactin F. Additionally, to determine the possible selectivity of the isolates toward infected erythrocytes, the two isolates were then

tested against two mammalian cell lines, i.e. human epidermoid carcinoma cells of the narsopharynx (KB) and breast cancer cells (BC), using ellipticine as a positive control. The isolates did not show the cytotoxic activity against both cell lines. The results indicated that the isolates presented selective toxicity against the *in vitro* growth of *P. falciparum* without affecting the mammalian cells. The selective action of 2'-deoxyadenosine towards *Plasmodium*-infected erythrocytes might partly be explained by the structural similarity to hypoxanthine, a precursor of purine base of *P. falciparum* through the purine salvage pathway. There is no report on the antimalarial activity of 2'-deoxyadenosine to date.

Table 29. Antimalarial activity* against *Plasmodium falciparum* K1, multidrug resistant strain and cytotoxic activity against KB and BC cells of macrolactin F (P035) and 2'-deoxyadenosine (S147)

Compounds	Antimalarial activity ED_{50} (μg/ml)[a]	Cytotoxic activity ED_{50} (μg/ml)[b]
macrolactin F (P035)	11.4	-
2'-deoxyadenosine (S147)	4.8	-

*Chloroquine diphosphate was used as a positive control.
[a]Data from hypoxanthine uptake method, chloroquine diphosphate was used as a positive control.
[b]Data from sulforhodamine B (SRB) colorimetric method, test at a concentration of 20 μg/ml, and ellipticine was used as a positive control.
KB = Human epidermoid carcinoma cell lines of the narsopharynx.
BC = Breast cancer cell lines.
ED_{50} = 50% effective dose.
- = Inactive.

4. Structure activity relationship (SAR)

A systematic structure activity relationship study of diketopiperazines, macrolactins, and 2'-deoxyadenosine were discussed as follows.

4.1 Structure activity relationship of diketopiperazines

The fermentation broth of each marine bacteria Sc004, Sc018, and Sc026 yielded eight diketopiperazines (DKPs). All of the isolated DKPs are cyclic dipeptides, which possess a proline moiety and the other amino acid, i.e. glycine, leucine, isoleucine, phenylalanine, and tryptophan. Anti-herpes simplex virus activity of the DKPs was not reported elsewhere. To understand structure activity relationships in the hope of designing an antiherpes agent, the DKPs were therefore, evaluated for *in vitro* anti-herpes simplex virus activity. The isolated DKPs exhibited strong inhibitory effect (50-70%) on *Herpes simplex* virus type I (HSV-I) and moderate inhibitory effect (25-50%) on *Herpes simplex* virus type II (HSV-II) *in vitro* at a concentration of 50 μg/ml, using acyclovir as a positive control (Table 30). Higher inhibitory activity against HSV-I than HSV-II was noted for *cyclo*-(D-prolyl-leucyl) (F019), *cyclo*-(D-prolyl-isoleucyl) (F017), *cyclo*-(*trans*-4-hydroxy-L-prolyl-L-phenylalanyl) (F018), *cyclo*-(L-prolyl-L-phenylalanyl) (dkp27), and *cyclo*-(L-prolyl-L-tryptophanyl) (P350). Among *cyclo*-(prolyl-phenylalanyl) and *cyclo*-(prolyl-tryptophanyl), the anti-HSV I activity of the LL configuration was more potent than the DL configuration. It was previously reported that the stereochemistry of D-proline-L-aromatic amino acid containing DKPs is in a folded conformation in which a planar aromatic ring (a benzene ring for phenylalanine moiety or an indole ring for tryptophan moiety) is folded over the diketopiperazine ring with the two rings nearly parallel and making van der Waals contacts (Westley *et al.*, 1968). The R_f values of *cyclo*-(L-prolyl-L-tryptophanyl) (P350), *cyclo*-(D-prolyl-L-tryptophanyl) (P352), *cyclo*-

(L-prolyl-L-phenylalanyl) (dkp27), and *cyclo*-(D-prolyl-L-phenylalanyl) (P348) on C-18 reversed-phase TLC, using THF:H_2O (3:7) as a mobile phase were 0.30, 0.38, 0.48, and 0.54, respectively. It could be concluded that the polarity of the LL configuration is less than that of the DL configuration. The conformation and the lipophilicity of the isolated DKPs might play a role in the virus penetration, or a suppression of viral binding to host cells (Vero cells) at an early replication stage (Hayashi *et al.*, 1997). The anti-herpes activity of the DKPs *in vitro* had highly specific structural and stereochemical requirements. However, the DKPs with decreased activity *in vitro* might appear to have favorable anti-herpes properties *in vivo*.

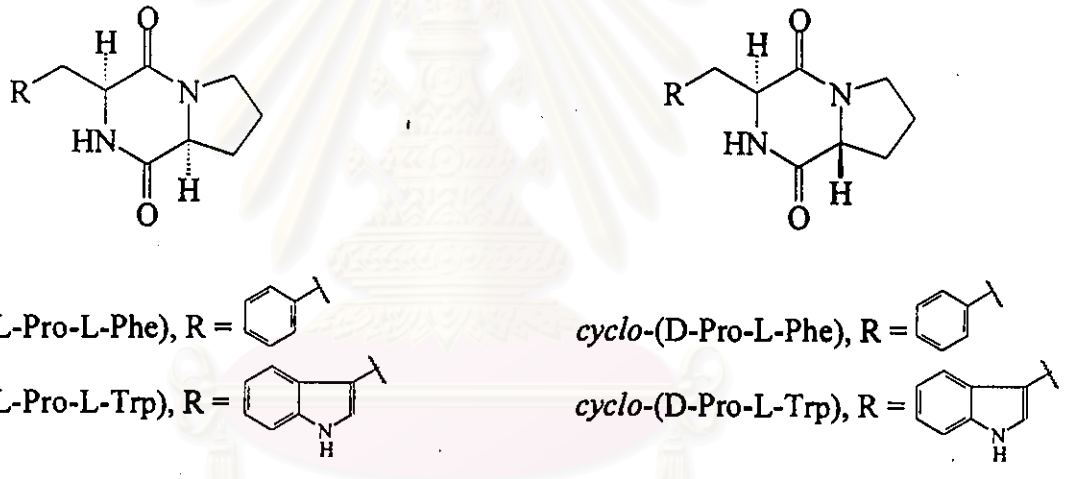

Figure 27. Structures of *cyclo*-(L-prolyl-L-phenylalanyl) (dkp27), *cyclo*-(D-prolyl-L-phenylalanyl) (P348), *cyclo*-(L-prolyl-L-tryptophanyl) (P350), and *cyclo*-(D-prolyl-L-tryptophanyl) (P352)

Table 30. Antiviral activity against *Herpes simplex* virus type I and type II of isolated diketopiperazines and synthetic diketopiperazine

Compounds	Anti-HSV I activity[a]	Anti-HSV II activity[a]
cyclo-(L-prolyl-glycyl) (P056WC)	++	++
cyclo-(L-prolyl-glycyl) (S142)	++	+
cyclo-(D-prolyl-leucyl)[b] (F019)	+++	+
cyclo-(L-prolyl-D-leucyl) (P049)	++	++
cyclo-(D-prolyl-isoleucyl)[b] (F017)	+++	+
cyclo-(*trans*-4-hydroxy-L-prolyl-L-phenylalanyl) (F018)	+++	+
cyclo-(L-prolyl-L-phenylalanyl) (dkp27)[c]	+++	+
cyclo-(D-prolyl-L-phenylalanyl) (P348)	++	++
cyclo-(L-prolyl-L-tryptophanyl) (P350)	+++	+
cyclo-(D-prolyl-L-tryptophanyl) (P352)	+	+

[a]Data from plaque reduction method.
Test at a concentration of 50 μg/ml.
Acyclovir was used as a positive control (100% inhibition).
- = inactive + = 25% inhibition
++ = 50% inhibition +++ = 75% inhibition
[b]Stereochemistry could not be determined.
[c]Synthetic compound.

Both synthetic DKPs including *cyclo*-(L-prolyl-L-tryptophanyl) and *cyclo*-(L-prolyl-L-phenylalanyl) were previously reported to possess inhibitory effects against gram-positive bacteria (*Staphylococcus aureus*, *Bacillus subtilis*, and *Streptococcus pneumoniae*) and gram-negative bacteria (*Escherichia coli*, *Pseudomonas aeruginosa*, and *Klebsiella pneumoniae*) (Milne *et al.*, 1998). However, the antimicrobial activity of

the isolated diketopiperazines and the synthetic diketopiperazine could not be tested due to the limited amount of samples available for biological studies.

4.2 Structure activity relationship of macrolactins

The preliminary studies showed that macrolactin F (P035), 7-*O*-succinyl macrolactin F (P129), and 7-*O*-succinyl macrolactin A (P103) exhibited antibacterial activity against *S. aureus* and *B. subtilis* using an agar diffusion method. The inhibition zones of macrolactin F (P035), and 7-*O*-succinyl macrolactin F (P129) against *S. aureus* were 28.0 and 8.0 mm, respectively, and against *B. subtilis* were 8.0 and 8.5 mm, respectively, at a concentration of 100 μg/disk (Table 31). The inhibition zones of 7-*O*-succinyl macrolactin A (P103) against *S. aureus* and *B. subtilis* were 24.0 and 10.1 mm, respectively, at a concentration of 50 μg/disk. The R_f values of macrolactin F (P035), 7-*O*-succinyl macrolactin F (P129), and 7-*O*-succinyl macrolactin A (P103) on a silica gel TLC, using $CHCl_3$:MeOH (85:15) as a mobile phase, were 0.64, 0.54, and 0.44, respectively. The results indicated that the order of polarity of macrolactins is 7-*O*-succinyl macrolactin A (P103) > 7-*O*-succinyl macrolactin F (P129) > macrolactin F (P035). The antibacterial activity against *S. aureus* of macrolactin F (P035) was more potent than of 7-*O*-succinyl macrolactin F (P129). The result indicated that a succinic acid half-ester moiety at C-7 might contribute to its hydrophilic property and sterically hindrance, which might interfere the transport mechanism through bacterial cell wall. However, 7-*O*-succinyl macrolactin A (P103) exhibited the most potent antimicrobial activity against *S. aureus*. It might be due to the presence of an additional conjugated diene, contributing to an effective conformation for the binding to biomolecules in bacterial cell.

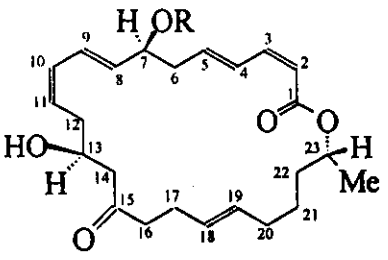

macrolactin F, R = H

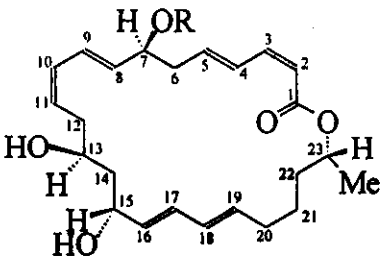

macrolactin A, R = H

7-*O*-succinyl macrolactin F, R = 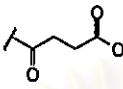

7-*O*-succinyl macrolactin A, R = 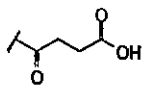

Figure 28. Structures of macrolactin F (P035), 7-*O*-succinyl macrolactin F (P129), macrolactin A, and 7-*O*-succinyl macrolactin A (P103)

Table 31. Antibacterial activity against *Staphylococcus aureus* and *Bacillus subtilis* of three isolated macrolactins using an agar diffusion method

Compounds	Concentrations (μg/disk)	Inhibition zones (mm)	
		S. aureus ATCC 25923	*B. subtilis* ATCC 6633
macrolactin F (P035)	100	28.0	8.0
7-*O*-succinyl macrolactin F (P129)	100	8.0	8.5
7-*O*-succinyl macrolactin A (P103)	50	24.0	10.1

In a previous report, macrolactin A showed anti-HSV I and anti-HSV II activities with the IC_{50} of 5.0 and 8.3 μg/ml, respectively (Gustafson, Roman, and Fenical, 1989). In this research, macrolactin F (P035), 7-*O*-succinyl macrolactin F (P129), and 7-*O*-succinyl macrolactin A (P013) isolated from the EtOAc extract of *Bacillus* sp. Sc026 exhibited anti-HSV I and anti-HSV II activities using a plaque reduction method (Table 32). All anti-HSV assays were tested at a concentration of 50 μg/ml. The known macrolactin A having two pairs of conjugated dienes (C-16 to C-19)

and a hydroxyl group at C-15, exhibited anti-HSV activity against both HSV-I and HSV II more potent than the isolated macrolactin F having a double bond (C-18 to C-19) and a carbonyl group at C-15. It might be suggested that the conjugated dienes (C-16 to C-19) and a hydroxyl group at C-15 are essential for exhibiting anti-HSV activity. The polar 7-*O*-succinyl macrolactin A (P103) showed anti-HSV I activity similar to the nonpolar macrolactin F (P035). The reduction of anti-HSV II activity of 7-*O*-succinyl macrolactin A (P103), compared to macrolactin F (P035) might be due to the succinic acid half-ester moiety at C-7. It might imply that the steric effect of this additional succinyl group interfere the binding effect between the macrolactone ring and the viral envelope of HSV-II. In addition, the hydrophilicity of 7-*O*-succinyl macrolactin A (P103) decreased the penetration of macrolactone ring through the envelope of HSV II. 7-*O*-Succinyl macrolactin F (P129) was inactive against both viruses.

Table 32. Anti-herpes simplex virus activity of three isolated macrolactins

Compounds	Anti-HSV I activity	Anti-HSV II activity
macrolactin F (P035)	+++	+++
7-*O*-succinyl macrolactin F (P129)	-	+
7-*O*-succinyl macrolactin A (P103)	+++	++

Data was obtained from a plaque reduction method using acyclovir as a positive control (100% inhibition) and compounds were tested at a concentration of 50 μg/ml.

- = inactive
+ = 25% inhibition
++ = 50% inhibition
+++ = 75% inhibition

4.3 Structure activity relationship of 2'-deoxyadenosine (S147)

Several modified purine nucleosides isolated from marine organisms showed anti-herpes simplex virus activity such as 9-β-arabinofuranosyladenine (araA, vidarabine) isolated from gorgonian, *Eunicella cavolini*, exhibiting highly effective antiviral activity against herpes viruses in human, including *Herpes simplex*, *Herpes zoster*, and cytomegalovirus (Cimino, Rosa, and Stefano, 1984). In this research, gram-positive marine bacterium Sc004 produced a known 2'-deoxyadenosine (S147), which was previously isolated from the tunicate, *Tridemnum cereum* (Dematte *et al.*, 1985) and the acorn worm, *Ptychodera flava* (Sakemi and Higa, 1985). It was inactive against HSV-I and HSV-II at a concentration of 50 μg/ml. The result might indicate that the hydroxyl group at C-2' of ribose moiety, as seen in 9-β-arabinofuranosyladenine, might be essential for anti-herpes simplex virus activity.

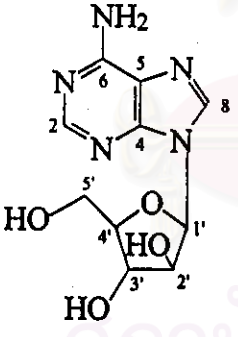

9-β-arabinofuranosyladenine

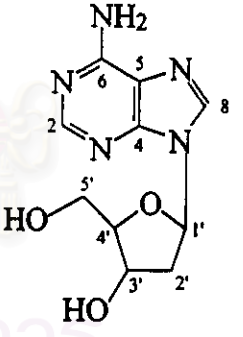

2'-deoxyadenosine (S147)

Figure 29. Structures of 9-*β*-arabinofuranosyladenine and 2'-deoxyadenosine (S147)